

**Design, analysis and optimization of lattice structure for additive  
manufacturing of aerospace components.**



By

Asadullah Jan

(Registration No: 00000361189)

Department of Mechanical Engineering

School of Mechanical and Manufacturing Engineering

National University of Sciences & Technology (NUST)

Islamabad, Pakistan

(2024)

**Design, analysis and optimization of lattice structure for additive  
manufacturing of aerospace components.**



By

Asadullah Jan

(Registration No: 00000361189)

A thesis submitted to the National University of Sciences and Technology,  
Islamabad,

in partial fulfillment of the requirements for the degree of

Master of Science in  
Mechanical Engineering

Supervisor: Dr. Adnan Munir

School of Mechanical and Manufacturing Engineering  
National University of Sciences & Technology (NUST)

Islamabad, Pakistan

(2024)

# THESIS ACCEPTANCE CERTIFICATE

## THESIS ACCEPTANCE CERTIFICATE

Certified that final copy of MS/MPhil thesis written by Regn No. 00000361189 Asadullah Jan of School of Mechanical & Manufacturing Engineering (SMME) has been vetted by undersigned, found complete in all respects as per NUST Statues/Regulations, is free of plagiarism, errors, and mistakes and is accepted as partial fulfillment for award of MS/MPhil degree. It is further certified that necessary amendments as pointed out by GEC members of the scholar have also been incorporated in the said thesis titled. **Design, analysis and optimization of lattice structure for additive manufacturing of aerospace components**


Signature: 

Name (Supervisor): Adnan Munir

Date: 13 - Feb - 2024

Signature (HOD): 

Date: 13 - Feb - 2024

Signature (DEAN): 

Date: 13 - Feb - 2024

---

Email: [info@nust.edu.pk](mailto:info@nust.edu.pk) Web: <http://www.nust.edu.pk>

Page: 1 / 1

2024/2/1



**National University of Sciences & Technology (NUST)**  
**MASTER'S THESIS WORK**

We hereby recommend that the dissertation prepared under our supervision by: Asadullah Jan (00000361189)  
Titled: Design, analysis and optimization of lattice structure for additive manufacturing of aerospace components be accepted in partial fulfillment of the requirements for the award of MS in Mechanical Engineering degree.

**Examination Committee Members**

- 1. Name: Muhammad Rizwan UI Haq      Signature:
  - 2. Name: Muhammad Salman Khan      Signature:
  - 3. Name: Izhar Ullah      Signature:
- Supervisor: Adnan Munir      Signature:

Date: 13 - Feb - 2024

13 - Feb - 2024

Head of Department

Date

**COUNTERSIGNED**

13 - Feb - 2024

Date

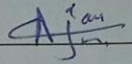
Dean/Principal

# CERTIFICATE OF APPROVAL

## CERTIFICATE OF APPROVAL

This is to certify that the research work presented in this thesis, entitled  
"Design analysis and optimization of Lattice Structure for AM of aerospace Component"  
was conducted by Mr./Ms. Asadullah Jan under the supervision of  
Dr. Adnan Munir

No part of this thesis has been submitted anywhere else for any other degree. This thesis is  
submitted to the S.M.M.E. (Name of Department of the University) in  
partial fulfillment of the requirements for the degree of Master of Science in Field of  
Mechanical (Subject Name)  
Department of S.M.M.E. National University of Sciences and Technology, Islamabad.

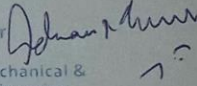
Student Name: Asadullah Jan Signature: 

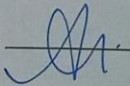
Examination Committee:

a) External Examiner 1: Name Signature: \_\_\_\_\_  
(Designation & Office Address)

b) External Examiner 2: Name Signature: \_\_\_\_\_  
(Designation & Office Address)

Supervisor Name: Dr. Adnan Munir

Signature:   
Dr. Adnan Munir  
Assistant Professor  
NUST School of Mechanical &  
Manufacturing Engineering,  
Islamabad, Pakistan

Name of Dean/HOD: Dr. Mian Ishfaq Ali Signature: 



## **AUTHOR'S DECLARATION**

I, Asadullah Jan hereby state that my MS thesis titled "Design, analysis and optimization of lattice structure for additive manufacturing of aerospace components" is my own work and has not been submitted previously by me for taking any degree from National University of Sciences and Technology, Islamabad or anywhere else in the country/ world.

At any time if my statement is found to be incorrect even after I graduate, the university has the right to withdraw my MS degree.

Name of Student: Asadullah Jan

Date: 13/02/2024

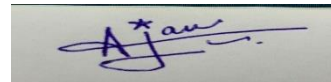
## PLAGIARISM UNDERTAKING

I solemnly declare that research work presented in the thesis titled “Design, analysis and optimization of lattice structure for additive manufacturing of aerospace components” is solely my research work with no significant contribution from any other person. Small contribution/ help wherever taken has been duly acknowledged and that complete thesis has been written by me.

I understand the zero-tolerance policy of the HEC and National University of Sciences and Technology (NUST), Islamabad towards plagiarism. Therefore, I as an author of the above titled thesis declare that no portion of my thesis has been plagiarized and any material used as reference is properly referred/cited.

I undertake that if I am found guilty of any formal plagiarism in the above titled thesis even after award of MS degree, the University reserves the rights to withdraw/revoke my MS degree and that HEC and NUST, Islamabad has the right to publish my name on the HEC/University website on which names of students are placed who submitted plagiarized thesis.

Student Signature: \_\_\_\_\_



Name: \_\_\_\_\_ Asadullah Jan

## **DEDICATION**

*Dedicated to my exceptional parents (Mr. & Mrs Jan Bahadur), adored sibling and respected friends for their unending love and support which lead to the completion of this thesis.*



## **ACKNOWLEDGEMENTS**

I am incredibly grateful to Almighty Allah, the most Generous, Merciful, and Kind One who gave me the fortitude and bravery to finish this research.

I acknowledge and appreciate the guidance and valuable suggestions of Dr. Adnan Munir and Dr. Aqeel Ahsan Khurram under whose supervision, this study has been completed. The author highly acknowledges their co-operation and friendly way of interaction which made this study joyful despite all the difficulties that were experienced. Beside these, I am thankful for the honorable GEC members Dr. Salman Khan, Dr. Rizwan ul Haq, Dr. Izhar Ullah and all the family and friends' prayers and help and last but not the least all the lab engineers and attendants that made this study possible.

## **Copyright Statement**

- The author retains the copyright for the textual content of this thesis. Reproduction, whether in full or in part, is permissible only in accordance with the author's provided instructions and must be lodged in the Library of NUST School of Mechanical & Manufacturing Engineering (SMME). For specific details, kindly consult the Librarian. Any reproductions must include this page. Additional reproductions, by any means, require the written permission of the author.
- Intellectual property rights related to any content described in this thesis are owned by NUST School of Mechanical & Manufacturing Engineering, unless a prior agreement states otherwise. Third-party use of such intellectual property requires written permission from the SMME, which will specify the terms and conditions of any agreement.
- For further details on the conditions governing disclosures and exploitation, please contact the Library of NUST School of Mechanical & Manufacturing Engineering in Islamabad.

# Table of Contents

THESIS ACCEPTANCE CERTIFICATE.....	ii
CERTIFICATE OF APPROVAL.....	iv
AUTHOR’S DECLARATION.....	v
PLAGIARISM UNDERTAKING.....	vi
DEDICATION.....	vii
ACKNOWLEDGEMENTS.....	viii
Copyright Statement.....	ix
Table of Contents.....	x
List of Figures.....	xii
List of Tables.....	xiii
Abstract.....	xiv
CHAPTER 1: INTRODUCTION.....	1
1.1 Background of Additive Manufacturing.....	4
1.2 Classification of AM Methods.....	5
1.2.1 Solid based AM.....	5
1.2.2 Powder Based AM.....	6
1.2.3 Liquid Based AM.....	7
1.3 Selective Laser Melting.....	9
1.4 Critical 3D printing parameters in SLM.....	11
1.5 Limitation of SLM.....	12
CHAPTER 2: METHODOLOGY.....	14
2.1 Model design.....	14
2.2 Lattice Structure for AM.....	15
2.2.1 Body Centered Cubic.....	16
2.2.2 Faced Centered Cubic (FCC).....	16
2.2.3 Gyroid Lattice Structure.....	17
2.3 Designing of Uniform and functionally graded structure.....	17
2.4 Specimen preparation.....	19
2.4.1 Compression specimen design.....	21
2.4.2 Bending specimen design.....	22
2.5 Materials and Methods.....	23
2.5.1 Titanium Alloy Material.....	23

2.6 Measurements of Mechanical Responses .....	25
CHAPTER 4. CONCLUSIONS AND FUTURE RECOMMENDATION .....	28
4.1 Compressive responses.....	28
4.2 Bending responses .....	30
4.3 Homogeneous lattice structure.....	31
4.4 Functionally graded lattice structure .....	32
4.5 Comparison between homogeneous and functionally graded lattice structures.....	34
4.6 Numerically Validation .....	36
4.7 Conclusion.....	40

## List of Figures

Figure 1:3D printed titanium parts: Hip joints, fan blade, rocket tip, titanium lattice component, titanium bracket, surgical spinal implant[21] .....	3
Figure 2:US-based Orthofix Medical’s 3D printed titanium implant Construx Mimi Ti Spacer System earned US FDA approval in 2021[21]. .....	3
Figure 3:Classification of AM techniques based on the type of base materials used[43].....	8
Figure 4: SLM technology's advantages over traditional techniques for producing biomedical devices [44].....	11
Figure 5: Fin CAD Model design .....	14
Figure 6:Uniform lattice structure of Fin Model .....	18
Figure 7:functionally graded lattice structure of Fin Model. ....	19
Figure 8: (a) BCC Unit Cell [68] (b) CAD Model of Homogenous lattice Three-point bending specimen (c) Functionally graded lattice Three-point specimen.....	20
Figure 9: CAD Model of Compression specimen, Fabricated specimen.....	21
Figure 10:(a) CAD model of three-point bending (b) fabricated specimen three-point bending.....	22
Figure 11:Farsoon FS421M machine for printing of test specimens through SLM[69].....	23
Figure 12: Tensile test Stress-strain curve. ....	25
Figure 13: As fabricated all BCC Lattice tests specimens. ....	26
Figure 14:All Test specimens after Testing.....	27
Figure 15: Experimental setup showing the direction of application of the Bending force.....	27
Figure 16:Stress-strain curve under compression for BCC lattice structure with experimental setup procedure from (a)-(e).....	29
Figure 17: Compressive stress-strain curves of BCC lattice structure..... <b>Error! Bookmark not defined.</b>	
Figure 18:Three-point bending tests curves of all three homogeneous lattice structure specimens. ....	31
Figure 19: Load-deflection curve of homogenous lattice structure with experimental step by step pictures (a) initial point (b) fracture in top facesheet (c) damaging core lattice structure (d) breaking of bottom facesheet.....	32
Figure 20:Three-point bending tests curves of all three functionally graded lattice structure specimens. .	33
Figure 21:Load-deflection curve of functionally graded lattice structure with bending test experiment set up (a) initial position (b) final position. ....	34
Figure 22:Uniform lattice structure average graph.....	35
Figure 23: Functionally graded structure average graph.....	35
Figure 24: Experimental and Numerical test specimens.....	36
Figure 25:Experimental and FEA curves of compression test .....	37
Figure 26:(a)-(e)Experimental compression test specimen behavior: From (f)-(j) compression specimen FEA.....	38
Figure 27:Experimental and FEA curves of three-point bending test.....	39
Figure 28:From (a)-(d) Experimental three-point bending test specimen setup: from (e)-(h) Numerical analysis of three-point bending test specimen. ....	40

## List of Tables

Table 1: The geometrical dimensions of BCC test specimens .....	20
Table 2: Material properties of Ti-6Al-4V. ....	24
Table 3: SLM process parameters for TiAl6V4 .....	25

## Abstract

Additive Manufacturing (AM) techniques, such as Selective Laser Melting (SLM), have gained significant attention in recent years by providing design freedom to engineers to design and fabricate complex cellular structures with tailored mechanical properties. To balance the strength and weight, 3D lightweight metallic Body-Centered Cubic (BCC) lattice sandwiches were fabricated by selective laser melting with titanium alloy (Ti6AL4V). This study investigates the mechanical responses under compression and three-point bending tests experimentally and numerically. The experimentally measured strengths are very close to the numerical predictions, demonstrating excellent mechanical properties. The numerical modelling may represent the stress-strain load-deflection curves, and the failure mode is the strut buckling initiated from the plastic hinges with high stress levels. This paper also explores the mechanical properties of functionally graded density BCC lattice structures, which results in different performances in mechanical behavior compared to uniform graded density BCC lattice structures. Due to the gradient lattice structure, the average bending load capacity significantly increases from 6000.0 N to 16000.0 N. We indicate that the BCC lattice structure only exhibits a dual failure model comprising buckling and fracture, in contrast to other lattice structures that often offer sole buckling or fracture failure. The buckling failure of the struts near the bottom face sheets always arises first and is followed by the subsequent fracture. The BCC lattice sandwiches offer an opportunity to effectively balance strength and weight as they present lower density than engineering alloys and higher strength than honeycombs, foams and pyramid lattice sandwiches.

Keywords: Additive manufacturing, Selective Laser Melting (SLM), Body Centered Cubic (BCC) Lattice Structures, Functionally Graded Density, Mechanical Properties



## CHAPTER 1: INTRODUCTION

Additive manufacturing (AM) has opened new horizons for the researchers to transform their concept into a functional model with customized properties or improved mechanical properties. In conventional AM, a structure is created, modeled, and designed using the computer-aided design (CAD) method. It is then divided into several thin layers, and material is added layer by layer, from bottom to top, utilizing an ultrasonic, laser, or electron beam to melt and combine the materials. [1]. Using computer-aided design (CAD), layer by layer construction of a three-dimensional object was initially accomplished through rapid prototyping, which was founded in the 1980s for the purpose of creating models and prototype components. This technology was developed to assist in realizing the visions that engineers have for their work.[2] Additive manufacturing is gaining industrial acceptance and altering how manufacturers handle problems based on research. For the AM of metallic components, many methods are now in use; the print-part quality, mechanical characteristics, component performance, and range of materials that may be produced are both advantages and disadvantages of these processes. Recently, Cellular core sandwich fabrication now has a possibility due to the quick development of additive manufacturing. In particular, AM was commonly used to create metal lattice sandwiches. Specifically, because of its great reliability and little porosity, Selective laser melting (SLM) is thought to be among the best production techniques [3] and is the method most frequently employed to create metal architectural structures [4]. Industry accepts SLM as a common method for producing intricate, valuable metal parts that are tailored for usage in biomedical, automotive, aerospace, and other fields [5-8]. SLM allows for high precision in creating complex geometry with good tolerance and built part layer by layer, forming strong, dense, and fully dense metal parts [9]. AM techniques have been considered an alternative to conventional manufacturing processes for the past few decades [10]. The main advantage that encourages their implementation on a large scale is said to be their ability to produce near-net form goods quickly from a variety of materials [11]. The majority of aerospace parts are produced using traditional techniques including forging, machine work, and others, where the final product contains less than 5% of the raw material [12]. While in the case of AM, maximum material utilization is of near net parts. The most popular geometric components created with additive manufacturing (AM) techniques include lattice structures, intricately curved shapes, and thin-walled structures [13].

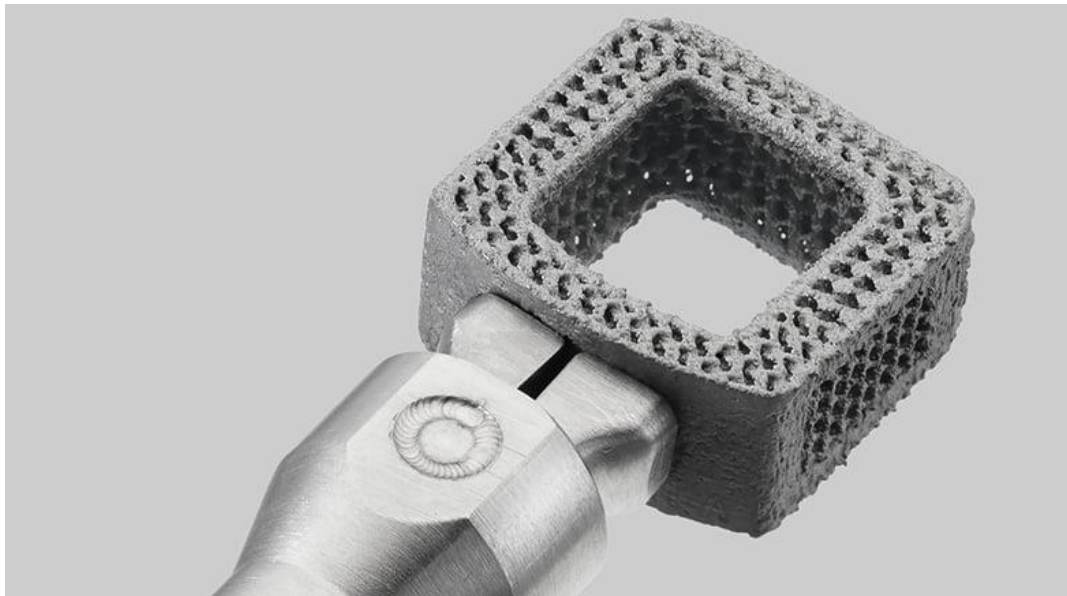
The technique of deliberately reducing mass while maintaining structural integrity and overall strength is known as lightweighting. With AM, you can now employ novel lightweight techniques to achieve even more mass reduction [14]. AM lightweighting may significantly lower production costs and emissions while enhancing ergonomics, performance, and energy efficiency. Using additive manufacturing to make items lighter results in more productive products for a variety of sectors [8, 14]. AM has multiple applications in the field of aerospace [8], defense [15],

automotive, and medical [16]—the aerospace industry benefits from additive manufacturing to produce lightweight, complex, and high-performance components. The aerospace sector utilizes additive manufacturing to create lightweight, complicated, and high-performing parts. The aerospace industry is one of the main sectors utilizing AM technology for testing, prototyping, and end-use component manufacture [17]. The world's top commercial airplane manufacturer, Airbus, also employed additive manufacturing to create its "Cabin bracket connector," which is constructed of titanium (Ti) powder and weighs more than 30% less than a machine- and mill-produced equivalent. This connector is used in the Airbus A350 XWB [18]. According to a new report, 12.3% of the worldwide additive manufacturing market was made up entirely of applications for aircraft. The study further predicts that AM Within the next 20 years, the sector is expected to develop from a \$1.5 billion business to a \$100 billion one, with the aerospace sector accounting for most of this expansion [19]. Lockheed Martin Space Systems Company reduces cost, cycle time, and material waste by using 3D printing technology to make titanium alloy satellite parts [20]. Rolls-Royce manufactured the 'front bearing housing' 3D printing technique using titanium. Within the Rolls-Royce Trent XWB-97 engine, the low and intermediate-pressure compressor bearing is housed in the front bearing housing. Compared to traditional manufacturing techniques, Rolls-Royce was able to reduce thirty percent of production time by utilizing this AM process [18]. Through additive manufacturing, the Australian Research Council (ARC) and Monash University have been advancing Australia's manufacturing sector. A \$9 million (AUD) investment from ARC has been made to highlight and support Australia's aerospace sector. The study group concentrated on tiny jet engine components composed of titanium alloy and produced using additive manufacturing. The study team discovered that engine components might be made more quickly and cheaply with 3D printing technology, which would also reduce weight and carbon emissions [15].

Below are some of lightweight additively manufactured by Selective laser melting from titanium alloy.



*Figure 1:3D printed titanium parts: Hip joints, fan blade, rocket tip, titanium lattice component, titanium bracket, surgical spinal implant[21] .*



*Figure 2:US-based Orthofix Medical's 3D printed titanium implant Construx Mimi Ti Spacer System earned US FDA approval in 2021[21]*

In aerospace, especially aviation, reducing weight is directly related to improving fuel efficiency. For a specific range profile, a lighter aircraft or spacecraft requires less fuel to be carried

[22]. Weight reduction is a conceptual challenge for engineers and designers, stimulating new developments in manufacturing processes, materials science, and overall vehicle design [23]. Weight reduction allows for a higher payload capacity [24]. This is crucial for space exploration since carrying more people, cargo, or scientific equipment may be constrained by the ship's weight. The weight of the spacecraft may be kept to a minimum, creating more room for valuable payloads. Lighter aircraft may travel longer or survive in flight for longer, which is vital for various aerospace applications [25]. Due to superior thrust-to-weight ratios, more lightweight aircraft can fly faster and at higher altitudes. During flight, a lighter aircraft experiences less stress on its structural parts, which might result in longer operating lifespans and fewer frequent maintenance requirements [26]. Lighter aerospace vehicles have less overall environmental effects since they use less fuel and emit fewer pollutants [8]. For aerospace manufacturing and research companies, achieving weight reduction can lead to a competitive advantage by offering more efficient and capable aerospace solutions [26, 27]. AM technology is best suited for aerospace applications because of the growing need for intricate and lightweight metal components, particularly from the aerospace industry [28]. Thus, this work aims to reduce the weight of aircraft fins by increasing strength to weight ratio. Compression, three-point bending and functionally graded three point bending test specimens were fabricated using SLM with titanium alloy (TiAl6V4), to explore the mechanical responses under the 3D Body Center Cube (BCC) lattice sandwich structure. An experimental and numerical testing was carried out, testing the above test specimens produced through the SLM process and using titanium alloy (TiAl6V4). The presented research is composed of 3 sections. The first section is design, which describes the designing technology and details of software to design the fin and test specimens. While the mechanical reactions, including failure modes and strengths, were covered in the second section. Lastly, section 3 provides a summary of the major findings.

## **1.1 Background of Additive Manufacturing**

Based on the ISO standard, AM technology was defined as “the procedure of combining materials to create items from a 3D model, often layer by layer; this approach contrasts with subtractive and formative manufacturing techniques”. In 1987, AM made its first commercial appearance with the Stereolithography technique. AM was originally known as rapid prototyping since its primary goal was to produce non-functional items, such as prototypes, due to the porosity and low strength features of the AM result. The potential of additive manufacturing (AM) to produce intricate structures with unparalleled design flexibility and rapid lead times has generated much attention and speculation, leading to ongoing progress and development in AM technologies[29].

Direct energy deposition (DED), powder bed fusion (PDF), material extrusion, material jetting, sheet lamination, binder jetting, and vat photopolymerization are the seven categories into which AM technologies may be divided[30]. Aspects of each AM method, including setups, materials, preprocessing, manufacturing, and post-processing, will be covered in this study. Since powder-based AM methods like DED and PDF are more widely employed, they will be examined in greater detail after that[31].

## 1.2 Classification of AM Methods

Classification of the AM method in this literature review is based on raw material. The varied physical states of the materials utilized in AM have varied qualities and traits[32]. The three states in which the materials are typically manufactured are dry powder, slurry/liquid, and solid-state. Figure 3 presents the categorization and lists the different material states that are used by distinct AM processes.

### 1.2.1 Solid based AM

Solid-based additive manufacturing, also known as solid-state additive manufacturing or solid-state 3D printing, is a subset of additive manufacturing techniques that use solid-state materials to construct items layer by layer. These materials are usually in the form of powders or filaments. Solid-based additive manufacturing uses materials that are already in a solid state, as opposed to some other types of additive manufacturing that use liquid or semi-liquid materials[33].

Using computer-aided design (CAD) software, a digital three-dimensional model is created to begin the process. The size and form of the thing to be made are specified by this model. Slicing software is used to divide the digital model into tiny horizontal layers. A cross-section of the object to be printed is represented by each layer[34]. The 3D printer is guided by a set of instructions produced by the slicing software, which is frequently in the form of G-code, on how to deposit material to create each layer. Thermoplastic polymers like nylon, ABS (acrylonitrile butadiene styrene), and PLA (polylactic acid) are commonly used in solid-based additive manufacturing. The extrusion system of the 3D printer is filled with the selected material's filament or pellets. The slicing software provides instructions that the 3D printer uses to move its nozzle along the X, Y, and Z axes. It glides across the build platform or previously printed layers, depositing small layers of molten material. The computer model determines the exact pattern in which the nozzle extrudes the material. The molten material swiftly cools and hardens as each layer is applied, connecting to the layer before it[33]. Until the complete item is produced, this layer-by-layer procedure is

continued. Support structures could occasionally be needed to provide overhanging elements stability when printing. Usually constructed of the same material as the item, these support structures are taken out once printing is finished. After printing is complete, the object may go through post-processing procedures including sanding or polishing rough surfaces, adding further finishes or coatings if needed, and removing any support structures. Many different sectors employ solid-based additive manufacturing extensively for end-use product creation as well as small-scale manufacture of sophisticated or bespoke parts. It has benefits including quick turnaround times, cheap cost, and the capacity to create complex geometries that could be challenging or impossible to do using conventional production techniques. It does, however, have several drawbacks, including a smaller resolution than other additive manufacturing methods and a smaller selection of materials[35].

### 1.2.2 Powder Based AM

Using a process called powder-based additive manufacturing (AM), often referred to as powder bed fusion, powdered material is deposited and fused in consecutive layers to form three-dimensional structures. This method is widely used because it can manufacture complicated geometries with great precision and resolution in a variety of sectors, including aerospace, automotive, and medical[36].

The first step of the procedure involves either 3D scanning an existing object or utilizing computer-aided design (CAD) software to create a digital 3D model. The additive manufacturing process follows the blueprint provided by this digital model. Slicing software is used to divide the digital model into tiny horizontal layers. The thickness of each layer usually varies from tens to hundreds of microns, based on the particular needs of the application and the tools being utilized. Powdered materials, including metals, polymers, ceramics, and composites, are used in powder-based additive manufacturing[37]. The selected material is fed into a recoater system or a build chamber, where it is dispersed equally across a build platform to create a thin coating. The powdered material is selectively melted or sintered using a high-precision deposition method, which frequently uses an electron or laser beam, in accordance with the sliced cross-section from the computer model. The powder particles are fused or bound together to produce the appropriate shape of the current layer by carefully controlling the energy source (laser or electron beam). The construction platform lowers, or the recoating mechanism applies a fresh layer of powder material once one layer is finished. For every layer, the selective deposition procedure is repeated, fusing the most recent layer to the oldest. This method of building an item layer by layer is followed until the full entity is created. The material rapidly cools and hardens as each layer is fused and deposited. This makes it more likely that the freshly deposited layer will stick to the older ones and keep its intended form. Following printing, the created product may go through a number of

post-processing procedures to enhance its dimensional accuracy, surface smoothness, or mechanical qualities. Depending on the particular needs of the application, this may involve surface coating, heat treatment, machining, or polishing[38].

### 1.2.3 Liquid Based AM

A subset of additive manufacturing techniques is called liquid-based additive manufacturing (AM), sometimes referred to as vat polymerization or vat photopolymerization. Liquid-based additive manufacturing (AM) creates objects by selectively solidifying liquid photopolymer resin, as opposed to typical additive manufacturing processes like fused deposition modeling (FDM) or selective laser sintering (SLS), which function by depositing or fusing material layer by layer[39].

Similar to other additive manufacturing (AM) techniques, liquid-based AM starts with the use of computer-aided design (CAD) software to create a digital 3D model. The shape and composition of the product to be produced are specified by this digital model. Thin horizontal layers, usually tens to hundreds of microns thick, are cut from the computer model. Each layer of the item is represented by a succession of 2D cross-sectional photographs created by this slicing procedure[40]. Liquid photopolymer resin is placed within a vat or reservoir for the printing process. Resin is a unique kind of liquid polymer that hardens when it comes into contact with a certain light wavelength, most often ultraviolet (UV) light. Lowering a platform into the resin vat is the first step in the printing process. The platform is fastened to an elevator mechanism or built platform that has vertical movement capability. The construction platform is coated uniformly with a thin coating of liquid resin as the platform lowers and dips into the resin. After the layer of resin has been spread out, certain regions of the resin that correspond to the cross-sectional form of the current layer of the item are selectively illuminated by a UV light source, such as a laser or a digital light processing (DLP) projector. The photopolymer resin hardens wherever the light hits, creating a thin coating of the item[39]. Depending on the particular machine and its parameters, the build platform climbs higher after a layer solidifies by an amount equal to the thickness of the subsequent layer, which is usually between 25 and 100 microns. Each layer is placed on top of the preceding layer after being selectively cemented in a repeating process. The item gradually emerges from the resin, layer by layer. The construction platform is lifted out of the vat and any extra resin is drained or removed when the printing process is finished. In order to get rid of any last bits of uncured resin, the printed item is usually washed in a solvent solution[41].

The printed object may go through additional post-processing steps, such as curing under UV light to fully harden the material, sanding or polishing to improve surface smoothness, or painting and



coating for functional or aesthetically pleasing reasons, depending on the particular application and desired surface finish. High resolution and fine detail capabilities, smooth surface finishes, and the capacity to create complicated shapes with intricate internal structures are just a few benefits of liquid-based additive manufacturing. It does have several drawbacks, though, such as fewer material options and slower construction times when compared to other AM techniques. All things considered, applications needing extreme accuracy and complex designs, such as dental prostheses, jewelry, and engineering and product development prototypes, are ideally suited for liquid-based additive manufacturing[42].

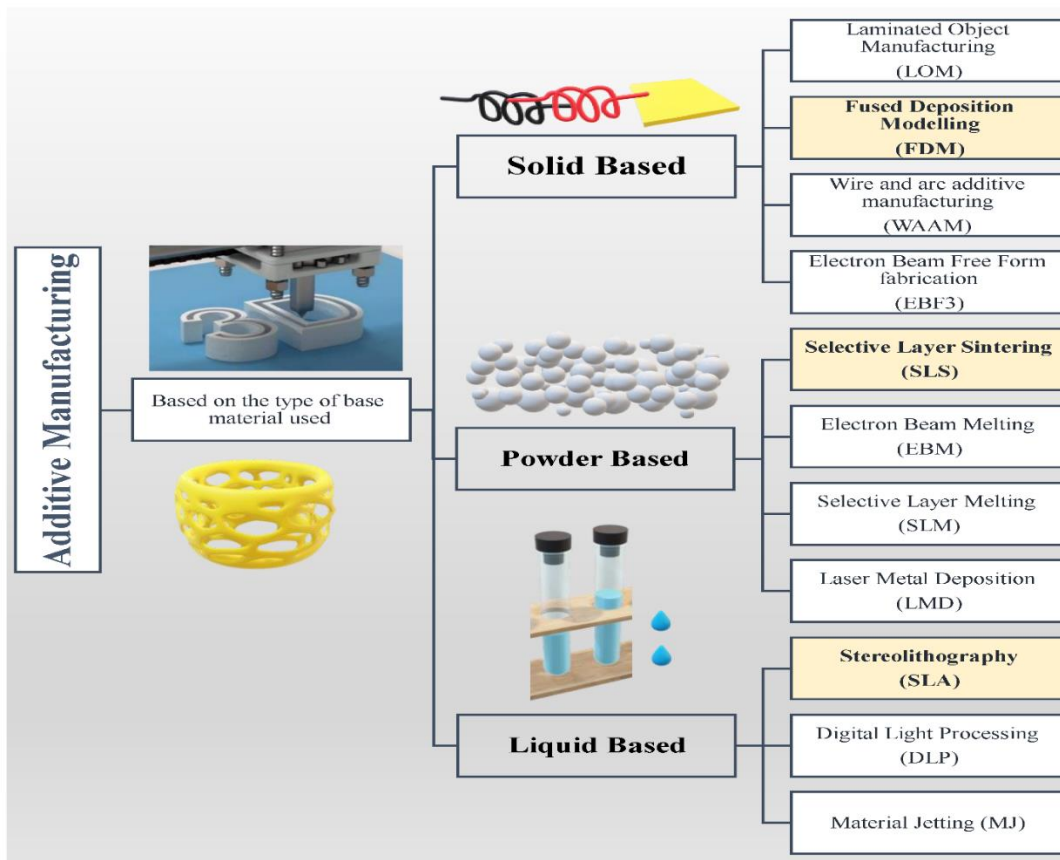


Figure 3: Classification of AM techniques based on the type of base materials used[43]

### 1.3 Selective Laser Melting

SLM was developed in 1995 by German researchers. The 3D printing technique is quite new. SLM forms 3D components using a powerful laser beam, much as SLA, which uses a UV laser[43]. Various metallic powders are melted and fused together by the laser beam during the printing process. The substance selectively connects or welds the particles together as the laser beam strikes a tiny coating of it. The printer builds upon its previous layer of powdered material by adding a new layer after a full print cycle. Next, the item is precisely lowered to equal one layer's thickness. When the print process is complete, the object will have any leftover powder physically removed. SLM employs fully melted powder, whereas SLS utilizes partly melted or sintered powder. This is the main difference between SLM and SLS. Final SLM products frequently have fewer or no voids, which increases their overall strength [43]. SLM printing is widely utilized for complex structures, thin walls, and sophisticated geometries in 3D products. In some of its creative endeavors, the aerospace industry uses SLM 3D printing. Typically, they are the ones who focus on precise, powerful, and lightweight components. SLM is currently widely utilized in the aerospace and orthopedics industries. Researchers, academic institutions, companies that create metal powder, and others that are eager to investigate the entirety of metal additive manufacturing's potential make investments in SLM 3D printers[43].

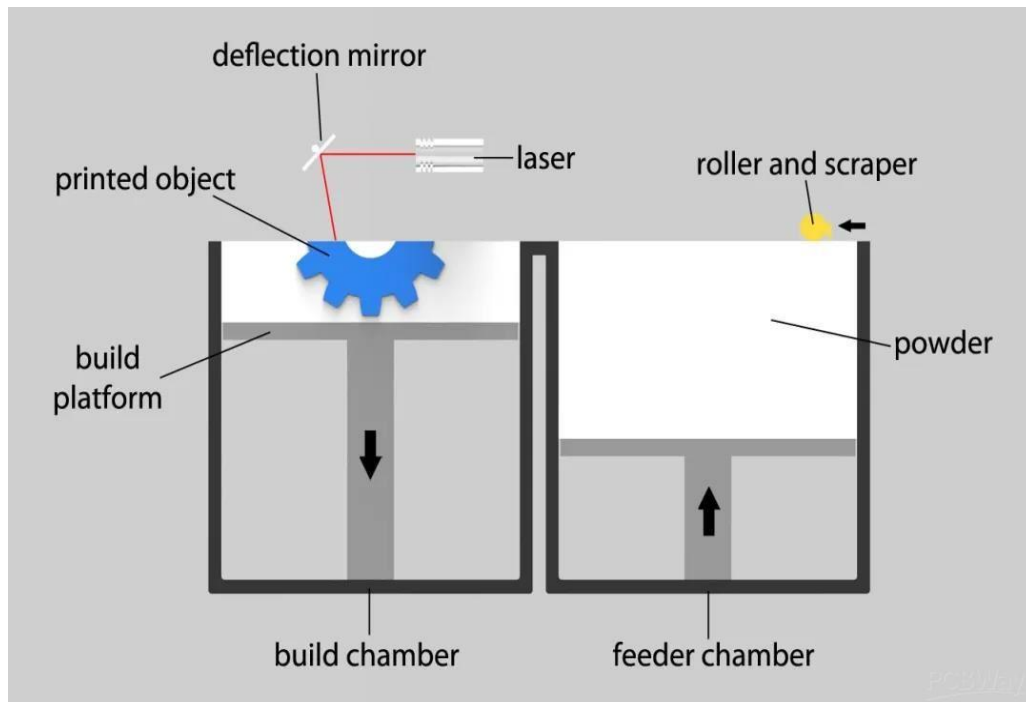


Figure 4: SLM process

Below are the advantages of SLM technology.

1. It enables the manufacturing of prototype device parts so that the design may be verified before going into mass production [44].

2. SLM technology enables low-volume manufacturing components, especially in the early design phase when it facilitates the prompt execution of design changes [45].

3. This technology, like other AM methods, ensures a quicker time-to-market for the created products by allowing for variable manufacturing phases, which reduces the length of the product life cycle[44, 46].

5. The production costs of biomedical equipment are immediately reduced by SLM fabrication, as it does not require expensive additional tooling or complicated assembly requirements [45].

6. Biomedical equipment may be freely customized and made more complicated via SLM technology[47].

Fig. 2 below illustrates the main benefits of SLM biomedical device manufacture over traditional manufacturing methods.



Figure 5: SLM technology's advantages over traditional techniques for producing biomedical devices [44].

#### 1.4 Critical 3D printing parameters in SLM

SLM is a metal additive manufacturing (3D printing) technique that builds up three-dimensional objects by selectively melting and fusing metallic powders layer by layer using a powerful laser. The effectiveness of SLM techniques is heavily dependent on several important elements. The following are some of the crucial variables:

- **Layer Thickness:** The printed object's resolution is determined by the layer thickness. Higher resolution is often achieved with thinner layers, although build times may rise[48].
- **Laser Power:** Laser power has an impact on the energy given to the powder bed, which in turn has an impact on the melting and consolidation of the metal powder. To guarantee correct melting without creating flaws, the ideal equilibrium must be found[48].
- **Scan Speed:** The laser beams scan speed is the rate at which it travels across the powder bed. Changes in scan speed can influence melt pool properties, heat input, and energy distribution[49].

- **Hatch Distance:** The distance between consecutive laser scan lanes is known as the hatch distance. It has an impact on the build's overall density and quality. Although it could take longer to build, a shorter hatch distance might boost part accuracy[49].
- **Powder Layer Uniformity:** For consistent melting and component quality, it is essential to provide an equal layer distribution of powder. Adequate methods for dispersing powder and oversight are crucial[50].
- **Build Chamber Atmosphere:** The build chamber's environment is regulated to keep the metal powder from oxidizing. It's normal practice to establish a safe atmosphere with inert gases like argon[48].
- **Material Powder Characteristics:** The size, distribution, and composition of the powder particles are significant factors. The quality and uniformity of the metal powder directly affects the mechanical properties of the final product [48].
- **Build Orientation:** The part's orientation on the build platform has an impact on the part's overall quality, support structure needs, and heat dissipation. Reducing distortion and enhancing mechanical qualities can be achieved by optimizing construction orientation[49].
- **Support Structures:** Suitable support structures are necessary to guarantee the stability of overhanging parts and to stop deformation during printing. Essential factors to take into account are the supports' design and removal after printing[50].
- **Cooling Rate:** To prevent cracking and guarantee appropriate metallurgical qualities, the pace at which the printed layers cool down is crucial. This may be achieved by changing the settings, which include laser power, scan speed, and others [48].
- **Post-Processing Parameters:** In order to get the required surface quality and material attributes, post-processing procedures like heat treatment and surface finishing could be required[49].

## 1.5 Limitation of SLM

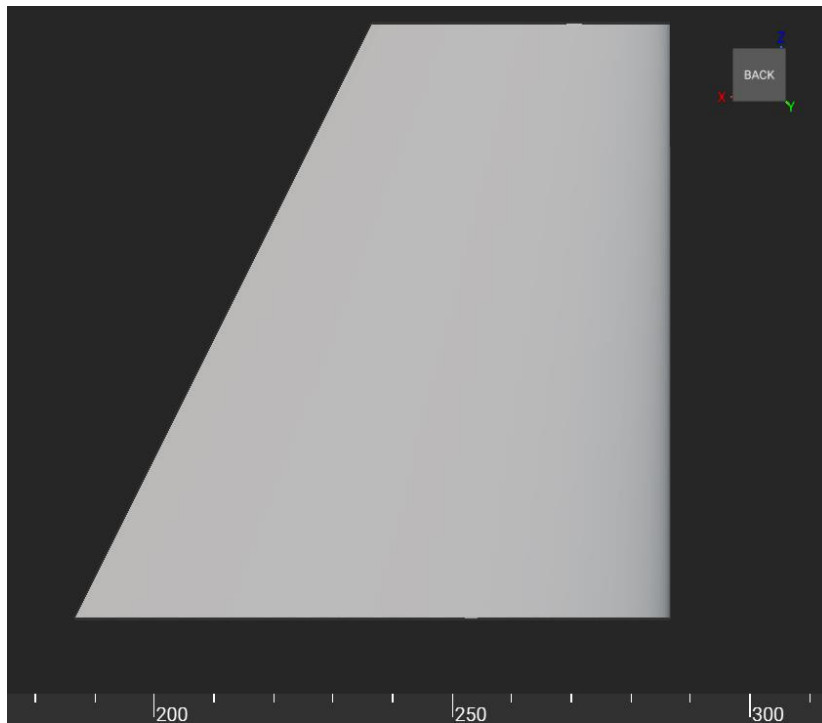
While SLM offers numerous advantages, it also has some limitations. Here are some of the key limitations of the SLM process:

- **Material Selection:** The main obstacle for SLM is the variety of materials that may be employed. Not all materials can be used in this technique, and there might not be as much supply of appropriate metal powders. A few characteristics of the material, including heat conductivity, may also affect the procedure[51].
- **Build Size:** When comparing SLM machines to traditional manufacturing processes, the build volume is frequently lower. The size of the pieces that may be created in a single construction may be limited by this constraint[52].

- **Surface Finish:** When SLM is used in place of conventional manufacturing methods, the components produced could have rougher surfaces polish. To get the right surface quality, post-processing operations like machining or polishing could be necessary[52].
- **Residual Stress and Warping:** Thermal gradients during the cooling process may cause the part's residual stresses to develop. This may cause warping or distortion, which would reduce the finished product's overall dimensional accuracy[52].
- **Support Structures:** Support structures are frequently needed in SLM to keep overhanging features from collapsing. Increased post-processing time may result from the time-consuming design and removal of these support structures after printing[51].
- **Cost of Equipment:** SLM machines may be costly to buy and operate, as can the related equipment. The initial investment cost may provide a limitation for smaller manufacturers or firms operating on a tight budget[52].
- **Design Constraints:** Due of limitations imposed by layer-wise deposition and process thermal properties, some design elements, including sharp corners and thin walls, may be difficult to achieve with SLM[51].

## CHAPTER 2: METHODOLOGY

The utilization of cellular lattice structures in the aerospace and military sectors is significant because of their high specific strength and stiffness. The parent material and architecture both affect the lattice structure's mechanical performance. BCC lattice structure has excellent performance in bending loads and has lower unit mass as compared to other lattice structures like FCC, gyroid etc. BCC lattice structure was used in fin design to minimize the mass and sustain the bending load.



*Figure 6: Fin CAD Model design*

### 2.1 Model design

Before the practical fabrication, the model of the aeroplane fin was well designed. For CAD geometry design, SolidWorks® is used to design solid geometry. The CAD geometry as shown Before the practical fabrication, the model of the aeroplane fin was designed. Using SolidWorks®[53] to design solid geometry as shown in **Error! Reference source not found.**(a). The CAD geometry was imported to nTopology[54] software for further processing. The design of the



fin was illustrated in the flowchart as shown in Error! Reference source not found.. The imported CAD body was converted into implicit and then it was shelled. The Shelled part subtracted from main body and BCC lattice structure was inserted. Both shell and lattice bodies were Boolean to make a single body. On that single body static structural simulation was performed.

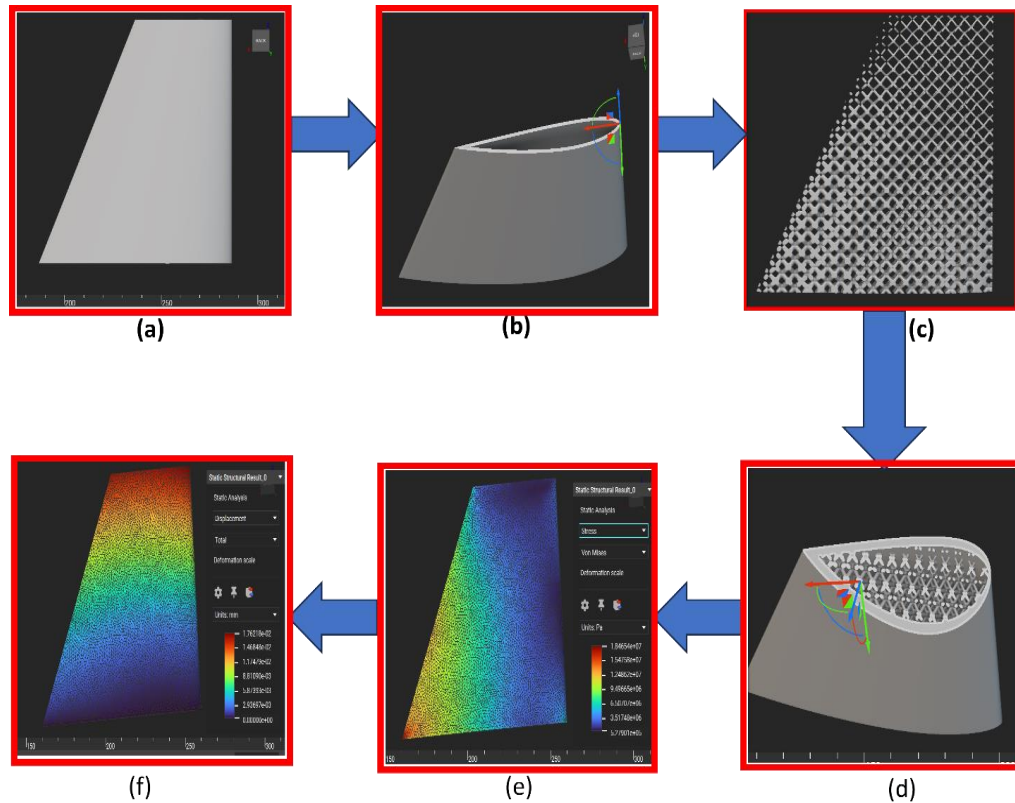


Figure 7: Flow chart Fin design

## 2.2 Lattice Structure for AM

An architecture known as a lattice structure is created by arranging unit cells with edges and faces in a variety of spatial arrangements. Both two and three dimensions are accessible for these cellular solids. For the most part Lattice structures are designed to offer solutions in a variety of industries, including the automotive, aerospace, and medical sectors[55]. They do this by combining improving properties like high energy absorption and reduced weight, which save manufacturing costs and time. These structures are more complex, making it challenging to design them using traditional CAD software[56]. Techniques for design synthesis are employed to create lattices. The porosity and relative density of the Lattice structure determine its superior mechanical

properties. Through several investigations, it is discovered that the structure's stiffness rises with relative density and that the lattice cellular materials affect the surface's roughness. The set of beam components or supporting struts attached to nodes forms the Lattice Cellular Materials. This fluctuates in a consistent manner with its volume and lattice boundaries. Lattice structure mostly consists of two topologies, periodic and stochastic. While the arrangement of cells along a single axis characterizes a periodic lattice structure, the dispersion of cells and their forms in a stochastic lattice structure follow an unsystematic probability distribution[57]. Although there are already about fourteen different kinds of lattices, researchers are still having trouble creating these lattice structures. Lattice structures may also be used to investigate the structural and compliance characteristics of materials at both micro and macro scales using a variety of tests, including axial, bending, torsion, and compression. The component's shape is resolved into mesostructured (structures of intermediate size and complexity) unit cells during these analyses[58].

### 2.2.1 Body Centered Cubic

A basic configuration of atoms or ions in solid materials, the Body-Centered Cubic (BCC) lattice structure is distinguished by a particular geometric pattern. Eight identically spaced neighbors encircle each lattice point in a BCC lattice, forming the cube's corners, with one extra atom at the cube's core[59]. Although it does not have direct touch with every nearby atom, the center atom shares space diagonals with all of them. Though not as densely packed as the face-centered cubic (FCC) lattice, this arrangement produces a high packing density when compared to simpler lattices like the basic cubic lattice. Many metals, including alpha iron at high temperatures, tungsten, chromium, and certain alloys like sodium and potassium, have the BCC structure[60]. Materials with this lattice structure have special qualities including excellent heat conductivity, high ductility, and toughness. Furthermore, it affects the way a material behaves under stress, which has an impact on characteristics like strength and deformation processes. A fundamental idea in materials science and engineering, the unique configuration of atoms in the BCC lattice is essential for defining the mechanical, thermal, and electrical characteristics of materials[61].

### 2.2.2 Faced Centered Cubic (FCC)

Along with BCC and hexagonal close-packed (HCP) structures, the face-centered cubic (FCC) lattice structure is one of the three most prevalent atom configurations in crystalline solids. Each lattice point in an FCC lattice has twelve nearest neighbors, which are positioned at the corners of a regular octahedron[62]. Six more distant neighbors that are situated at the centers of the octahedron's faces encircle each lattice point. Because of this configuration, the lattice's total coordination number is 12, meaning that every atom is in touch with 12 of its neighbors. A cubic

unit cell with lattice points at each face's center and each corner defines the FCC lattice[63]. The FCC structure is frequently found in metals including aluminum, copper, gold, and silver as well as in some non-metallic compounds like lithium fluoride because of its high symmetry and effective atom packing. The FCC structure is widely used in engineering applications ranging from structural materials to electrical conductors because of its many beneficial qualities, which include high ductility, strong thermal conductivity, and a very close-packed atomic arrangement. The FCC structure also has isotropic qualities, which means that all crystallographic orientations display the same physical characteristics. This makes it especially well-suited for applications that need uniform performance regardless of orientation[57].

### 2.2.3 Gyroid Lattice Structure

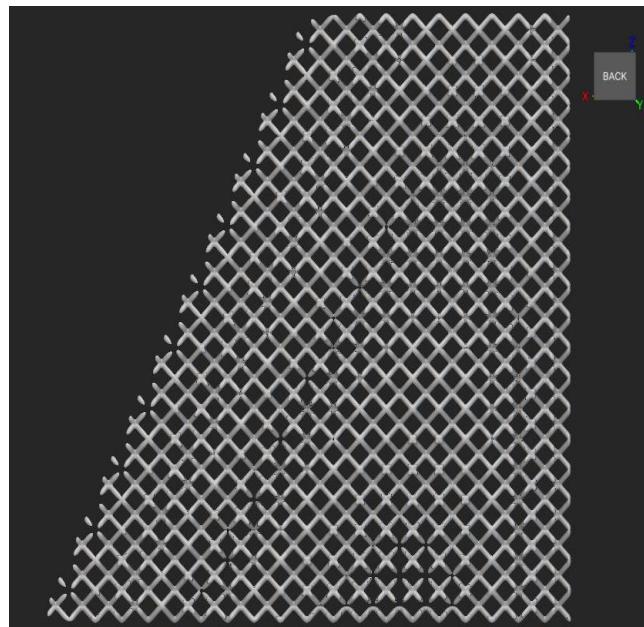
The complicated geometric design of the Gyroid lattice structure gives it unique features, making it a complex three-dimensional lattice[64]. This lattice structure is named for the mathematical word "gyroid," which characterizes a minimum surface that is triply periodic. Its network of interwoven, interconnecting channels forms a continuous, porous structure. Its topology creates a labyrinthine network with no dead ends, resembling a network of linked twisting and curved surfaces[65]. The Gyroid lattice's remarkable mechanical qualities, such as its high strength-to-weight ratio, outstanding stiffness, and impact resistance, are a result of its intricate geometry. Because of these qualities, it is very well suited for a wide range of technical applications, especially in the areas of innovative materials, biomimetic designs, and lightweight structural components[66]. Furthermore, the porous structure of the Gyroid lattice allows for effective heat transfer and fluid movement, which makes it useful in heat exchangers, filtration systems, and other applications needing improved transport qualities. The Gyroid lattice is a viable contender for pushing the limits of material science and engineering and expanding additive manufacturing processes because of its unique mix of lightweight design, structural integrity, and efficient material consumption[67].

## 2.3 Designing of Uniform and functionally graded structure

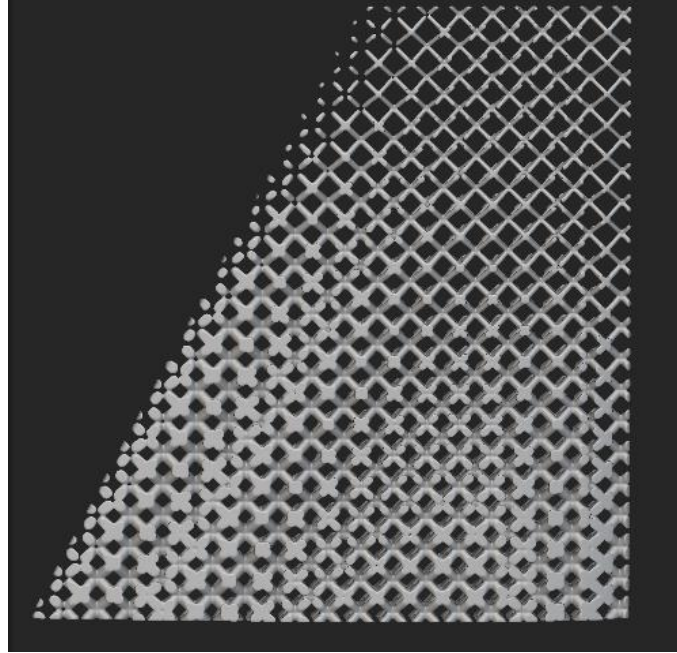
In three dimensions, a composite material or structure with a repeating pattern of components placed regularly is referred to as a uniform lattice sandwich structure. In engineering and materials science, this kind of structure is frequently utilized to attain mechanical qualities, such strength, stiffness, and light weight. A repeating unit cell, or a little section of the lattice that is repeated across the whole structure, makes up the structure. The strength-to-weight ratio and energy absorption are two examples of the attributes that the unit cell is made to maximize. In three dimensions, the lattice elements are set up uniformly and regularly. The total attributes of the

material may be expected and controlled with the assistance of regularity in the arrangement. The lightweight nature of lattice structures is one of its main features, which is advantageous for applications like the aerospace and automobile sectors where weight is a crucial issue. Uniform lattice density structure (shown in **Error! Reference source not found.**(a)) was inserted into the Boolean subtract body and make it combined to make a single body. Static structural analysis was performed on uniform lattice density body.

A functionally graded lattice density structure in 3D refers to a three-dimensional material or object with a lattice structure that varies in density across its volume in a controlled and intentional manner. The term "functionally graded" indicates that certain of the material's qualities are purposefully varied. Density is the variable characteristic in this situation. In various areas of the lattice structure, the density varies progressively or methodically. Lattice structures are configurations of geometric forms or cells that recur, creating a pattern that resembles a grid throughout a substance. Because of these structures' strength and small weight, they are often employed in materials science and engineering. Functionally graded lattice structure is a change in a structure's structure relative to its volume. Functionally graded lattice structure was designed, and static structural analysis was performed. Functionally graded lattice structure shows excellent results in bending load and displacement as compared to uniform density lattice structure.



*Figure 8: Uniform lattice structure of Fin Model*



*Figure 9: functionally graded lattice structure of Fin Model*

## 2.4 Specimen preparation

Periodic lattice structures comprise unit cells schematically repeated in space, so the unit cell is taken as the RVE of the lattice structure. As shown in **Fig 3a**, a typical unit cell of BCC configuration consists of 8 diagonal struts of equal length. To define the BCC unit cell topology, the following parameters are required: unit cell length ( $l_u$ ), strut diameter ( $d$ ), lattice angle ( $\theta$ ), and strut length ( $2l$ ). It is known that the mechanical properties of lattice sandwiches are mostly obtained under compression and three-point bending loads. According to our fin functionally graded lattice model design shown in **Fig. 1b**, we have designed two types of three-point bending test samples named uniform density lattice and functionally graded density, as shown in **Fig. 3b,3c**. The corresponding models of the specimens have bottom and top facesheets with the same thickness, the same specimens' height and width, and different lengths for compression and three-point bending.

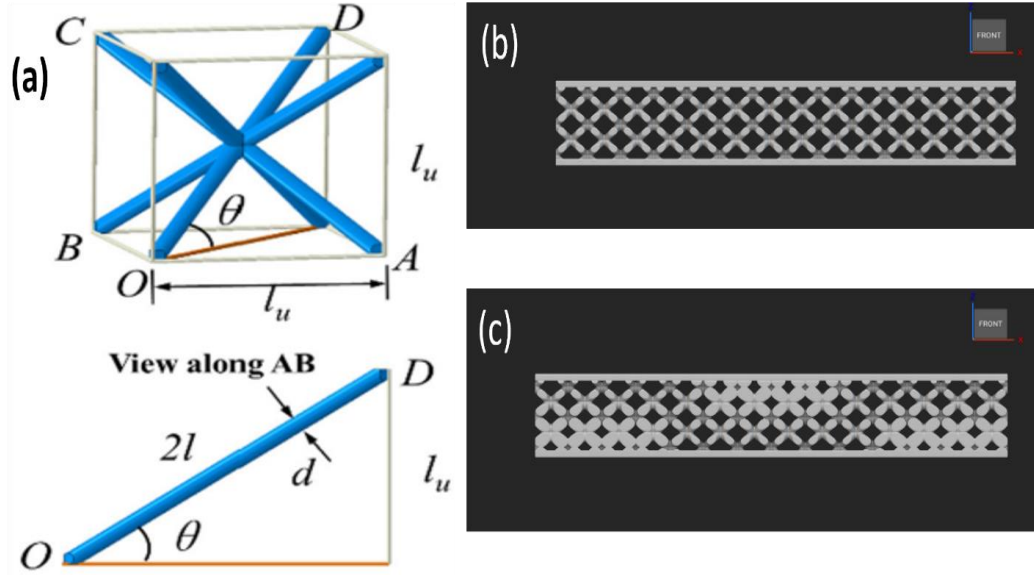


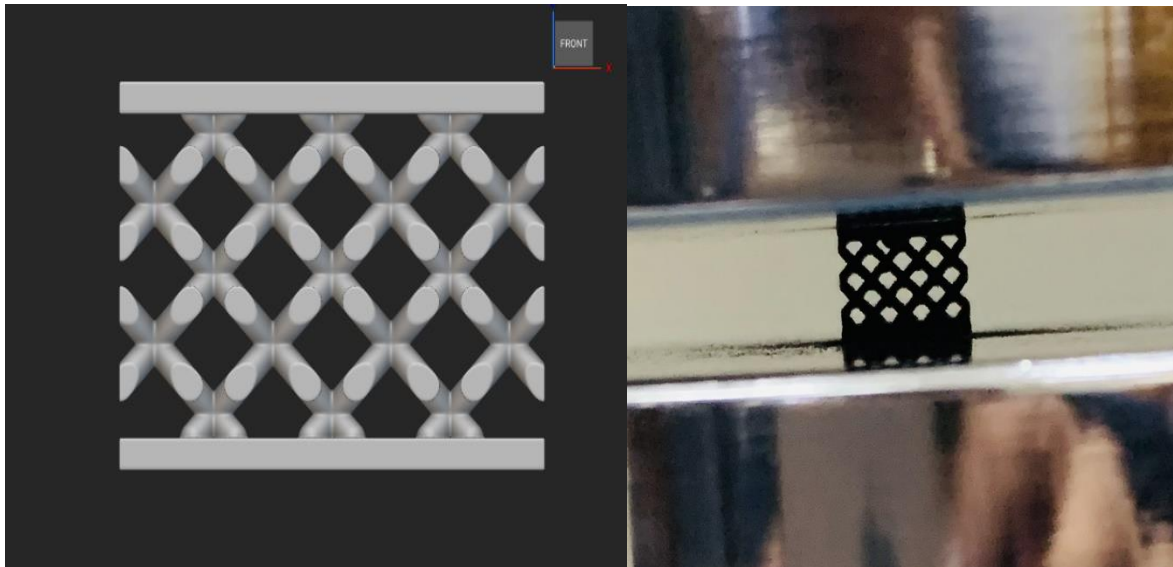
Figure 10: (a) BCC Unit Cell [68] (b) CAD Model of Homogenous lattice Three-point bending specimen (c) Functionally graded lattice Three-point specimen.

Table 1: The geometrical dimensions of BCC test specimens

Test specimen	d(mm)	$l_u$ (mm)	( $^\circ$ )	t(mm)	W×H (mm <sup>2</sup> )	$L_c$ (mm)	$L_B$ (mm)
Compression test	0.8	3.5	5	0.8	12.5 × 9.7	12.6	49.5
Three-point bending	0.8	3.5	5	0.8	12.5 × 9.7	12.6	49.5
Functionally graded three-point bending	0.5-1.5	3.5	5	0.8	12.5 × 9.7	12.6	49.5

### 2.4.1 Compression specimen design

A material having a Body-Centered Cubic (BCC) lattice structure is put to axial compressive forces in a compression test to see how it responds mechanically. In the field of materials science and engineering, the BCC lattice structure is frequently seen at low temperatures in metals. Compression test specimens for titanium alloy with a body-centered cubic (BCC) lattice structure can be designed using various software tools, including nTopology. nTopology is a computational design software allowing advanced geometry creation and manipulation. Three compression specimens were designed using nTopology with the geometry shown in **Fig 4**. Using ASTM C365 standard, the specimen was designed as  $L \times H \times W = 12.6 \text{ mm} \times 9.7 \text{ mm} \times 12.6 \text{ mm}$  with a strut diameter of 0.8 mm and thickness of 0.8 mm for up and bottom facesheets as the values of all parameters are listed in Table 1. Securely mount the specimen in the testing apparatus, such as a universal testing machine (UTM), making sure that the axial loading is applied along the axis of the specimen. Gradually apply an axial compressive load to the specimen at a controlled rate. The rate of loading is often specified in standards or based on the requirements of the experiment. Analyze the stress-strain curve to extract important mechanical properties, such as yield strength, ultimate strength, modulus of elasticity, and others. Summarize the results in a report, including any observations, conclusions, and insights gained from the compression test.



*Figure 11: CAD Model of Compression specimen, Fabricated specimen.*



## 2.4.2 Bending specimen design

The three-point bending test is a common method used to evaluate the mechanical properties of materials, including those with a BCC lattice structure. A machine that delivers a load at two sites and supports the specimen at a third is usually used to apply a specimen to a bending force in this test. Evaluating the material's behavior under bending stress is the aim.

Flexural testing is used to evaluate the mechanical properties of materials, specifically their bending strength and stiffness. The specimens typically consist of a rectangular bar with a specific geometry allowing controlled bending. As shown in Fig 2b, the three-point bending test specimen of uniform lattice density with a total length of 49.5 mm, width of 12.6mm, and height of 9.7mm as specified in ASTM C393 standard. As to compare the mechanical performance of uniform and graded density lattice structures, a functionally graded density lattice structure of a three-point bending specimen, as shown in **Fig. 2c**, was designed using the same ASTM C393 standard with a varying strut diameter of 0.5mm minimum and 1.5mm maximum. The values of all remaining parameters were kept the same as a three-point bending test specimen of uniform density lattice. Apply a load at the center of the specimen using the testing machine. The load should be applied gradually to avoid sudden failures. Measure and record the applied load and the corresponding displacement or strain during the test.

Monitor the behavior of the specimen, including any visible signs of deformation or failure. Calculate the stress and strain in the specimen based on the applied load and displacement data.

Analyze the load-displacement curve to identify key mechanical properties, such as the yield strength, ultimate strength, and modulus of elasticity. Observe and document the failure mode of the specimen. This could include yielding, plastic deformation, or fracture.

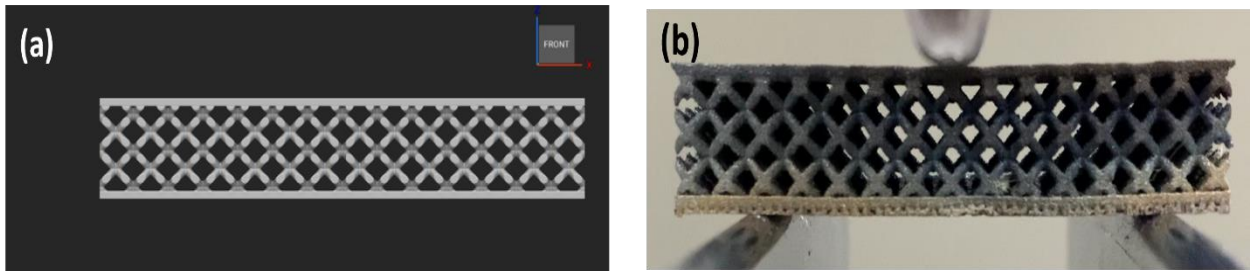


Figure 12:(a) CAD model of three-point bending (b) fabricated specimen three-point bending.



## 2.5 Materials and Methods

The SLM (Selective Laser Melting) process is used to fabricate metallic 3D BCC lattice sandwiches with titanium alloy. The procedure, which involves melting metallic powders under laser irradiation to create 3D structures layer by layer, was carried out utilizing Farsoon FS421M [69] equipment. The procedure comprised selectively melting Ti6Al4V powder layers that were repeatedly layered on a Ti6Al4V substrate in line with the data from the CAD model. Powdered Ti6Al4V gas atomized in a spherical form with a diameter varying from 15 to 50  $\mu\text{m}$  was the raw material employed. The protective gas used was argon. The process parameters are listed in **Table 2**. The scanning route was chosen to be zigzag. The fabricated 3D BCC lattice tests specimens were presented in **Fig. 6(a)** and **Fig.6(b)** shows specimens after performing of testing. Due to their unique and complex shape, the lattice structures were not polished after the remaining raw particles were removed by abrasive blasting.



*Figure 13:Farsoon FS421M machine for printing of test specimens through SLM[69]*

### 2.5.1 Titanium Alloy Material

Titanium alloys are regarded as a combination of high-tensile strength and toughness titanium plus a few chemical components. With characteristics that prevent corrosion, they can tolerate extremely high or low temperatures. Because of their composition, these light alloys are categorized as  $\alpha$ ,  $\alpha+\beta$ , and  $\beta$  kinds. For permanent implants in many biomedical applications, it is considered the gold standard due to its exceptional strength, resistance to corrosion, and

biocompatibility. Applications for titanium alloys may be found in the following fields: aerospace, orthopedics, dentistry, medical implants, and vehicles. An estimated 80% of titanium alloys are wrought and used in various applications.

However, titanium alloys also provide other significant benefits that have been recognized and are being used in a variety of non-aerospace applications. The metal possesses several notable attributes, such as its remarkable corrosion resistance, low thermal coefficient of expansion, strong creep resistance, high temperature strength, and relative abundance in the earth's crust. Titanium alloys have obvious advantages, but they are outweighed by the high component prices resulting from high metal extraction and shape and forming costs. Even in the historically performance-driven aerospace industry, production costs are predicted to play a significant factor in material selection going forward.

*Table 2: Material properties of Ti-6Al-4V.*

Ti-6Al-4V Mechanical Properties		
Properties	Values	Units
Melting Point	1604-1660	°C
Tensile Stress at break	1170	MPa
Compressive Strength	1070	Mpa
Elongation at break	10	%

Table 3: SLM process parameters for TiAl6V4

Parameter	Laser power	Laser spot	Scanning speed	Layer thickness	Hatch space
Value (TiAl6V4)	280W	100 $\mu\text{m}$	1200 mm/s	30 $\mu\text{m}$	80 $\mu\text{m}$

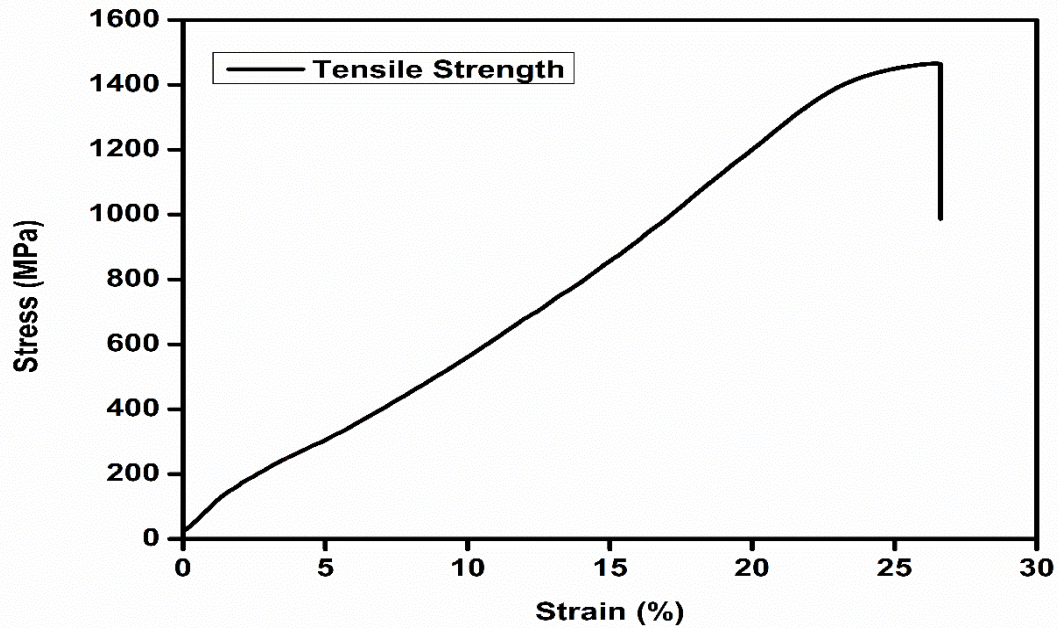
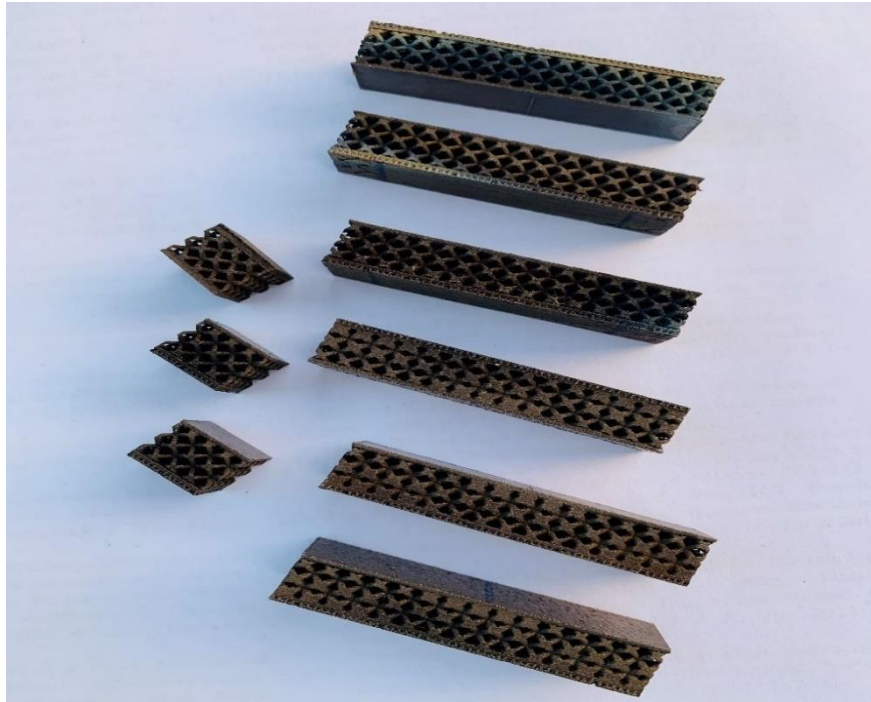


Figure 14: Tensile test Stress-strain curve.

## 2.6 Measurements of Mechanical Responses

Regarding the mechanical response measurement, a universal testing machine (HAIDA HD-B607-S) as shown in Fig 7, was used to measure the mechanical response experimentally under tensile, compression, bending loading cases. The titanium alloy produced by SLM was evaluated in accordance with ASTM E8/8M for its tensile response[70]. Standard test procedures for metallic material stress testing were followed for evaluating the specimen. The tensile test's stress-strain curve is displayed in Figure 5. Very similar findings to those published in the literature were achieved for the yield strength ( $\sigma_s = 1300.0 \text{ MPa}$ ) and Young's modulus ( $E=95.0 \text{ GPa}$ )[71]. Tensile

characteristics achieved here are somewhat less than those of Ti6Al4V produced by traditional forging because SLM will unavoidably introduce micro flaws such interlayer voids and unmelted raw powders. As per ASTM C365, a compressive force of 2 mm/min was applied to the BCC lattice sandwiches during the compression test using Instron 5985 [72]. The testing machine's sensor captured the deformation during the compression test.



*Figure 15: As fabricated all BCC Lattice tests specimens.*

In order to assess mechanical parameters including strength, stiffness, and deformation behavior, the three-point bending test of Ti6Al4V involves applying a load to a standard specimen, measuring the resulting deflection, and analyzing the results. This test is essential for determining if the material is appropriate for a certain technical application and assuring the reliability of the final product. Functionally graded and three point bending mechanical measurements were conducted according to ASTM C393 [73]. The force sensor determined the applied load, and the loading speed was 2 mm/min. A dial indicator that was mounted at the specimen's bottom

registered the deflection under bending. A digital video camera recorded the specimens' failure models and deformation evolutions during the testing.



Figure 17: All Test specimens after Testing.

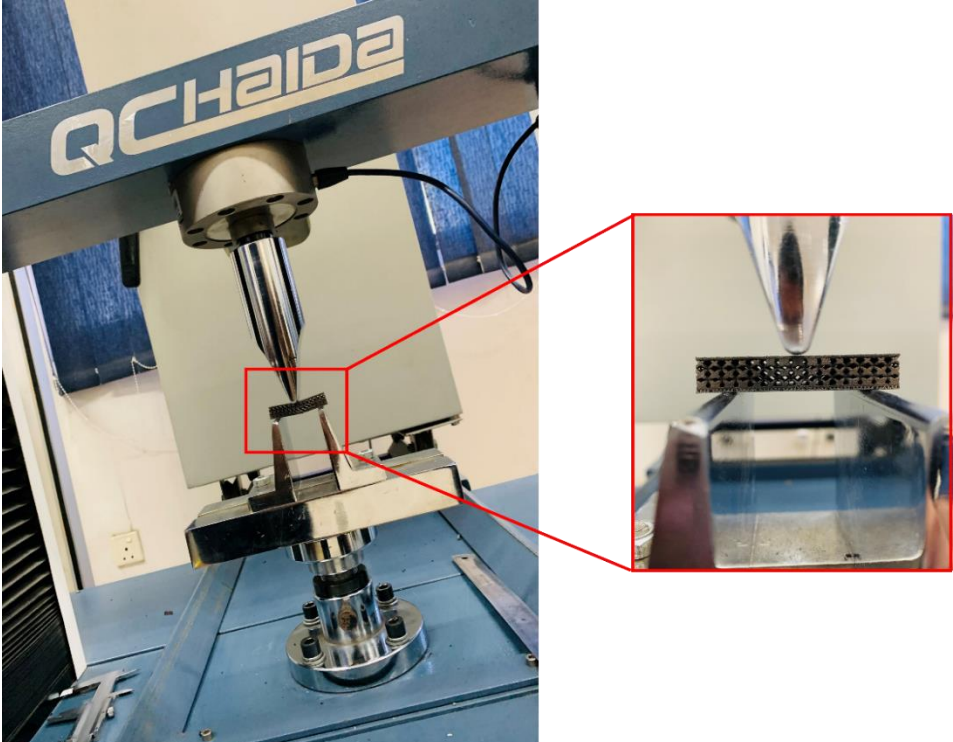


Figure 16: Experimental setup showing the direction of application of the Bending force.

## CHAPTER 4. CONCLUSIONS AND FUTURE RECOMMENDATION

### 4.1 Compressive responses

Compression tests were used to identify the effective stress-strain curves with respect to the compressive responses of the BCC lattice sandwich compression specimen. **Fig.8** illustrates the average stress-strain behavior of compression tests with experimental photos. As shown in **Fig.8a** the downward compressive load was applied on compression specimen, as a result, the stresses rise linearly to the first peak. At this stage the BCC lattice core sustains the load linearly up to highest peak, and the yield stress is obtained. The primary method of deformation is evidently the buckling of the struts in the vicinity of the top and bottom facesheets. The struts close to the facesheets in the region depicted in **Fig. 8b** begin to lose energy and decrease quickly to relatively low levels. The compressive specimen design shown in **Fig.4** has multiple layers of BCC lattice structure, so due to those layers the stresses increase again as these layers bearing the compressive load further. The curve rises again from region **Fig.8c** to the next peak. The specimen holds this plateau region and resists compressive up to maximum strain. As summarized in **Fig.8c-e**, finally the BCC lattice core completely fractured and loses the load capacity as curve drops rapidly downward.

**Figure 9** summarizes the effective stress-strain curves obtained from compression trials. All the curves show excellent consistency and follow the same trends having sharp peaks and plateau regions. These patterns imply that the experiments were successful, and the fabrication was reliable.



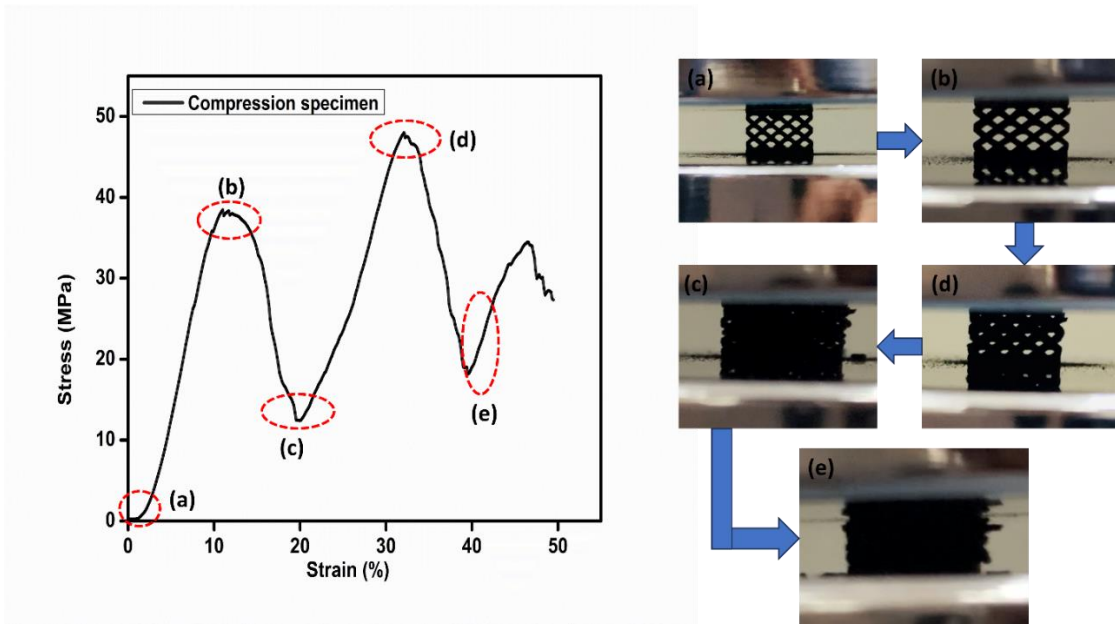


Figure 18: Stress-strain curve under compression for BCC lattice structure with experimental setup procedure

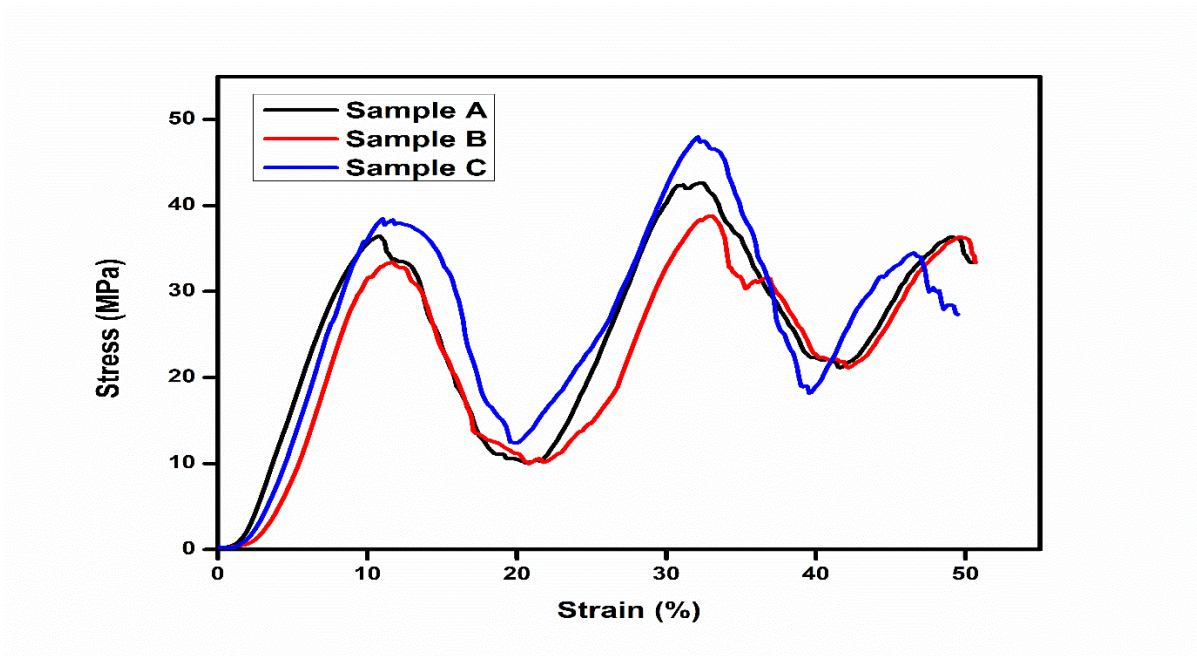


Figure 19: Compressive stress-strain curves of BCC lattice structure.

## 4.2 Bending responses

In this section, the three-point bending test is briefly explained as a mechanical test used to evaluate the flexural strength of materials. In order to cause bending, a load is given to the sample's center while it is supported by two supports. The sample experiences tension on one side, compression on the other, and a neutral axis in the middle as a result of the bending moment produced by the three points of contact. Crucial details on the material's mechanical behavior may be learned from how it reacts to three-point bending. To ascertain the flexural strength of the functionally graded lattice structures and the homogeneous lattice structure, tests were conducted. A load-deflection curve is commonly used to illustrate the correlation between the applied force and the associated deflection of the sample. At first, the material experiences elastic deformation when the force is applied, resulting in a linear curve. Plastic deformation may happen beyond a particular point, resulting in a non-linear portion in the curve. The material deforms reversibly under force in the elastic area, and the sample returns to its initial shape when the stress is released. The material's stiffness or modulus of elasticity is correlated with the slope of the linear component of the load-deflection curve. Plastic deformation happens when the applied load is greater than the material's elastic limit, causing the material to permanently distort. The yield point is the term used to describe the starting point of plastic deformation. A significant consideration in three-point bending is the maximum load that the material can support. The material could break down with higher loads. Depending on the material, failure mechanisms may include fracture, delamination, or other types of structural failure. Bending stress and strain distributions across the sample can be analyzed to understand how the material responds to the applied bending moment. The outer fibers of the sample experience maximum stress, and the inner fibers experience less stress.



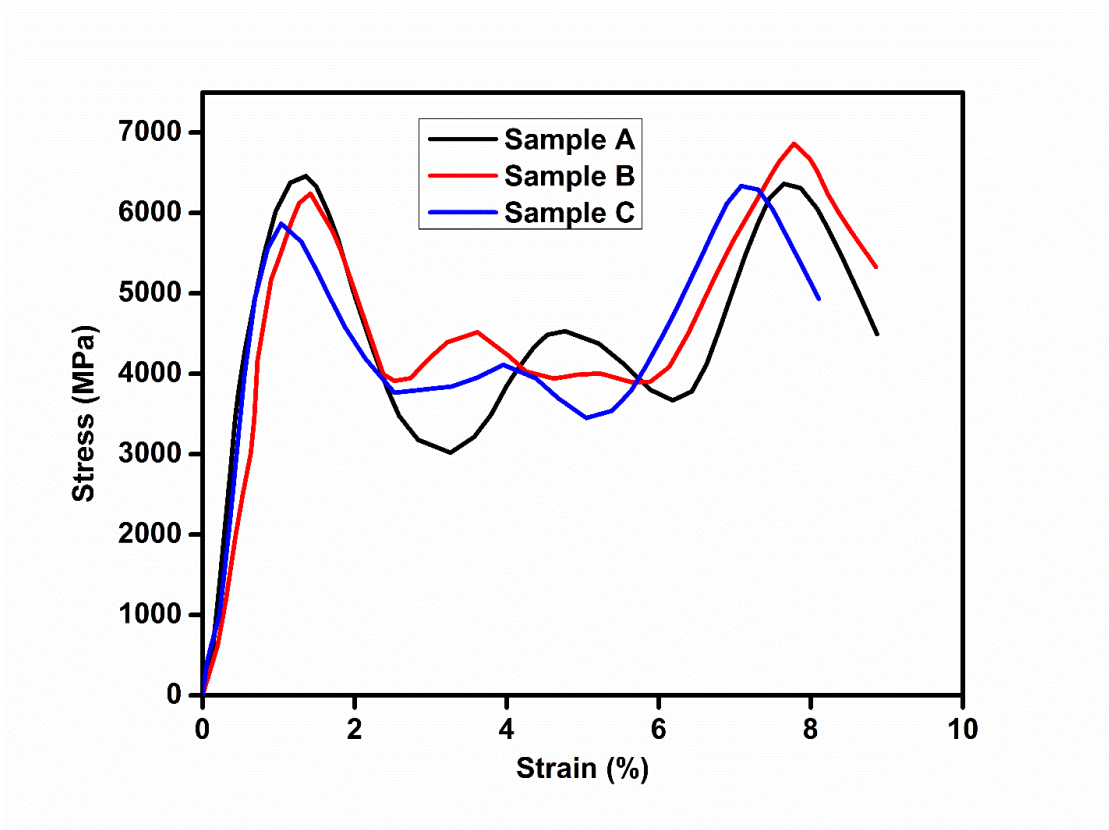


Figure 20: Three-point bending tests curves of all three homogeneous lattice structure specimens.

### 4.3 Homogeneous lattice structure

Regarding the bending responses, three point bending mechanical measurements were conducted according to ASTM C393. The load-deflection curves of all three specimens under bending experiments are summarized in **Fig.10a**. All the three curves have a linear sharp peak and a sinusoidal plateau region and finally, sharp rise till fracture. Overall, for a homogeneous lattice density, the curves for repetitive samples present excellent consistency, suggesting the reliability of the fabrication and effectiveness of the experiments. The bending deformation evolutions are illustrated in **Fig. 11a-d**. At the initial stage as shown in Fig.11a the load is just applied on the top facesheet which holds the load for certain time with no deformation but after certain time the facesheet starts deforming very slowly. The bending load linearly increases to the highest peak due to the strength of the top facesheet of homogenous lattice structure specimen. As present in Fig.11(b) the graph suddenly drops to the lowest level due to the fracture of facesheet. After that the BCC lattice structure sustains the load and the curve holds a wide range of plateau region due to layer-by-layer BCC lattice structure in the core of specimen. In Fig.11(c) the plateau region

shows the sinusoidal behavior just because of different BCC lattice structure bearing the buckling load and after large buckling deformation, the curved struts are finally fractured, and the core completely loses the load capacity. As shown in fig.8d the core is completely compacted, and bottom facesheets synchronously suffer buckling, and the curves correspondingly reach just one peak. After large buckling deformation, the homogenous lattice structure specimen is completely fractured. All specimens were fully damaged near the area where the force was applied. The highest compression force occurs in that specific area due to the bending of the specimens.

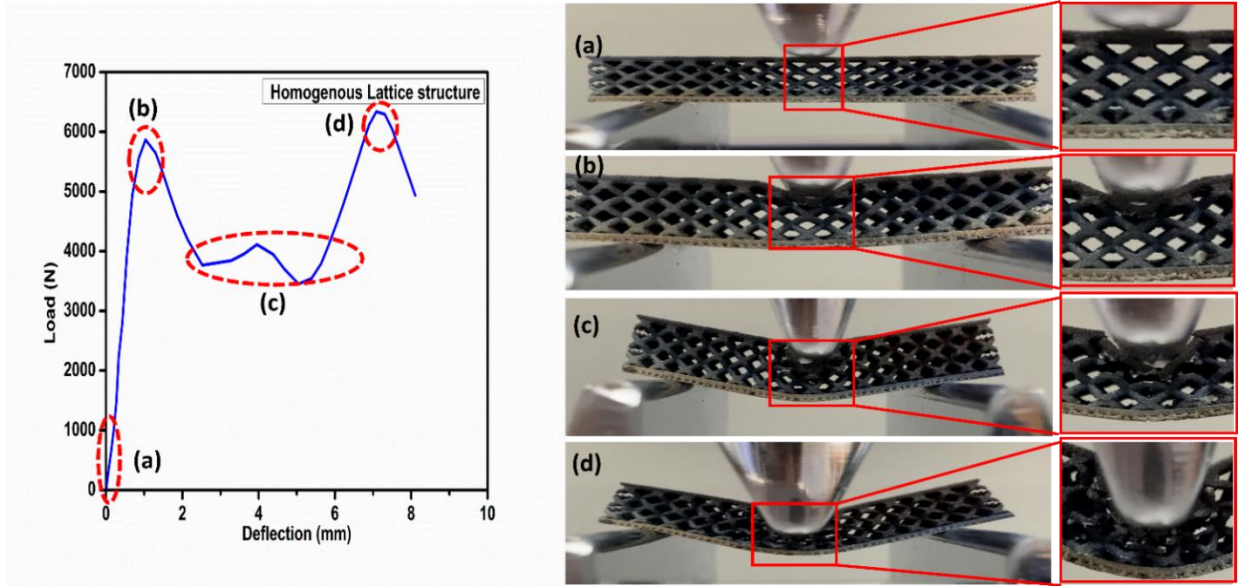


Figure 21: Load-deflection curve of homogenous lattice structure with experimental step by step pictures (a) initial point (b) fracture in top facesheet (c) damaging core lattice structure (d) breaking of bottom facesheet.

#### 4.4 Functionally graded lattice structure

**Figure 10** shows graphically the bending response of homogenous and graded lattice, which shows that increase in strut thickness behaves rigidly. All the functionally graded lattice structure specimens have very low buckling deformation as compared to homogenous. As shown in **Fig.10b** the curves linearly increase up to the highest peak and finally the curved struts fractured. In **Fig.12**, the graph and photos are presented to show the results of the three-point bending test on the functionally graded lattice structures. The results in the functionally graded lattice structure graphs look different from homogenous lattice structure due to the change in lattice density in the core of the specimen. At the initial stage as shown in **fig.12a** the bottom facesheet bears the bending load and the rises linearly up to its first highest peak. As compared to homogenous lattice structure this

specimen shows greater load bearing due to variation in lattice density. The lattice density is higher at three points where the load is applied and two support points. These various lattice structures sustain the bending load and very low deformation is shown. The load is gradually increasing downward from the middle point of the top facesheet, and the functionally graded lattice structure specimen is resisting the bending load to highest values of 16000 N. In **Fig.12b** the large bending force finally fractured the lower core portion of the specimen with bottom facesheet failure. This is due to the higher density lattice structure at the top and supports points. It has been observed that homogenous lattice structure shows greater buckling deformation while functionally graded specimens show more rigid behavior. These fractures demonstrate that the most vulnerable struts and nodes are followed by the crack. Changes in unit cell structure and strut thickness can cause different fracture behaviors [74]. The intersection of struts and nodes, that are the locations where stress concentrations occur, is often where the failure point of homogeneous and graded lattice specimens forms [75].

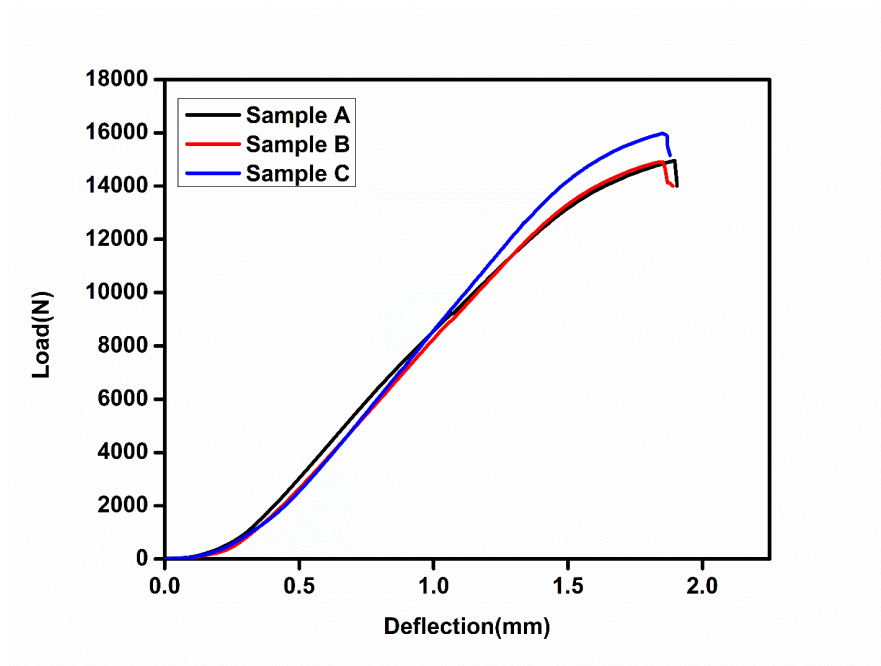


Figure 22: Three-point bending tests curves of all three functionally graded lattice structure specimens.

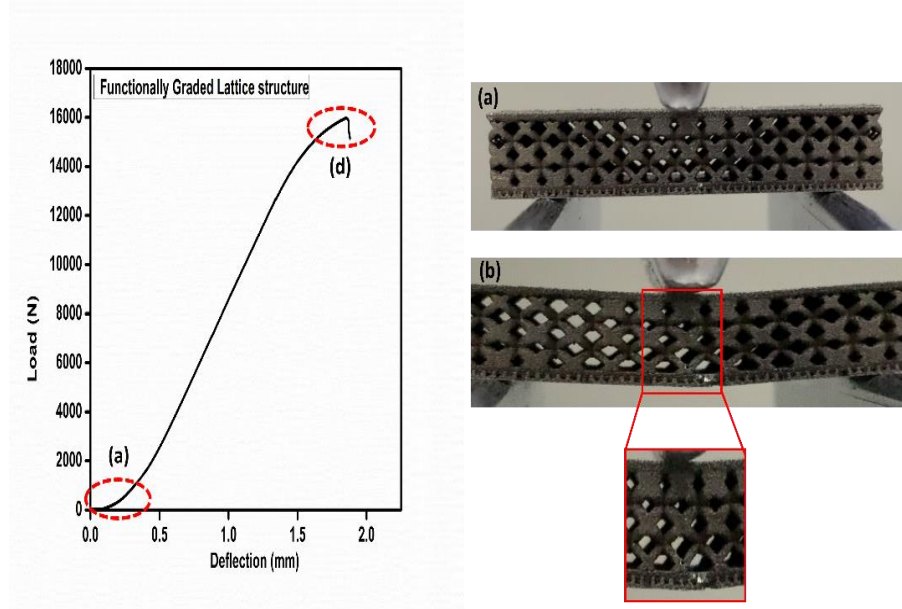


Figure 23: Load-deflection curve of functionally graded lattice structure with bending test experiment set up (a) initial position (b) final position.

#### 4.5 Comparison between homogeneous and functionally graded lattice structures

Homogeneous and functionally graded lattice structures are two types of materials or structures that differ in terms of their composition and properties. The experimental force-displacement properties of two sandwich constructions under three-point bending are shown in **Fig.11** and **12**. The results show that homogenous structures have high amount of buckling deformation due to its core lattice design, On the other hand, the functionally graded sample exhibits characteristically brittle behavior, with roughly linear stiffness until catastrophic collapse. In **Fig.10** both curves have different behavior just because of its unique lattice core design inside sandwich structures. As designed for good strength and stiffness, functionally graded force-displacement curves show excellent response to its strength and stiffness. Although homogenous structures have lower value of force-displacement but excellent behavior in energy absorption and buckling deformation.

In summary, the particular needs of the application will determine whether to use a homogeneous or functionally graded lattice structure. Functionally graded structures give an opportunity to customize material characteristics for improved performance under a variety of situations, although homogenous structures are more straightforward and economical. A trade-off between manufacturing considerations, performance optimization, and design complexity is frequently involved in the choice.



Below are the graphical comparison of uniform and functionally graded lattice structure:

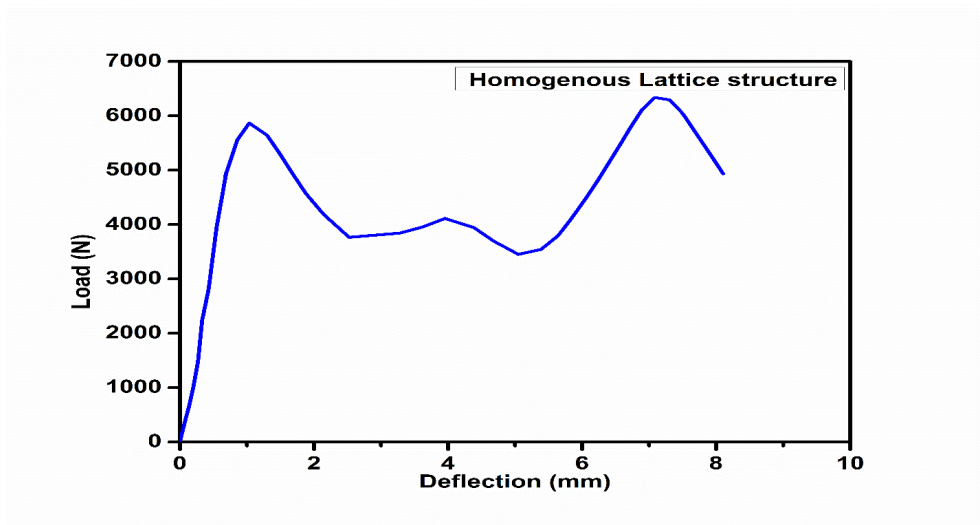


Figure 24: Uniform lattice structure average graph

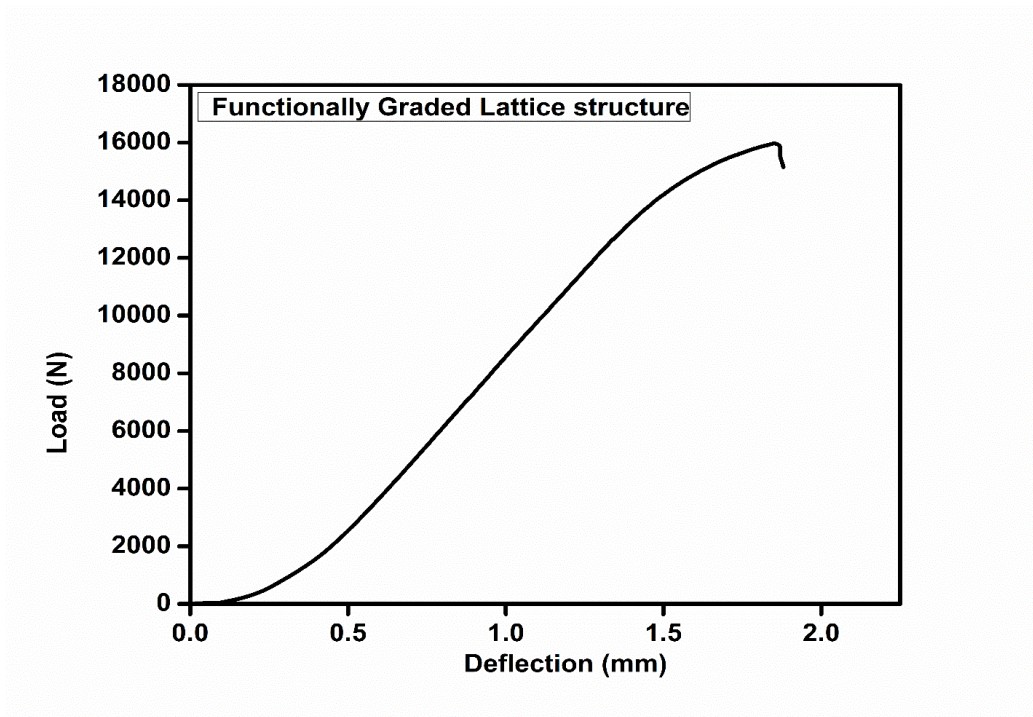


Figure 25: Functionally graded structure average graph

## 4.6 Numerically Validation

In engineering, a numerical technique known as finite element analysis (FEA) can be utilized to simulate how systems or structures will respond to certain conditions. It is frequently used to break down a physical structure into smaller, more manageable components known as finite elements in order to examine and solve complicated engineering challenges. These components are joined together at locations known as nodes to produce a mesh that depicts the system's overall shape. ANSYS 19.2 was used for all designs' FEA in order to numerically model the compression and three-point bending trials. The tests shown in Fig. were replicated with identical geometrical dimensions, molds, boundaries, and loading conditions. SolidWorks software was used to create the 3D model of the compression and three-point bending test specimens. The simulation was then run after importing the model into ANSYS Workbench. The elastic-plastic material model, which can represent the plastic deformation in the numerical modeling, was fed data on the Young's modulus, Poisson's ratio, yield strength, and actual plastic stress and strain. Both the stiff foundation and the bending supports were completely restricted for compression. Next, compressive and bending stresses were applied to the rigid punches by loading them vertically. In order to get reliable mesh-independent results, struts were fitted with a fine mesh, resulting in the generation of 35000 and 90000 elements respectively in the compression and bending FEA models. The failure mechanism—which could not be ascertained and investigated by experimental measurements—and the development and distribution of stress were acquired using numerical modeling. The relationship between loading force versus deformation and the failure modes that were depicted were the only things that could be measured experimentally. The failure modes, load-deflection curves, and nominal compressive stress-strain were analyzed numerically. Figure 13 displays the experimental configuration and FEA model for the bending and compression tests.


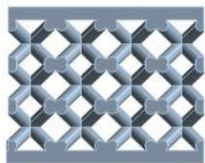

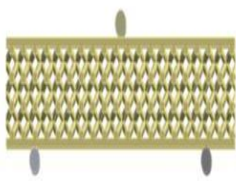
Test	Experiment	FEA
Compression		
Three-point Bending		

Figure 26: Experimental and Numerical test specimens

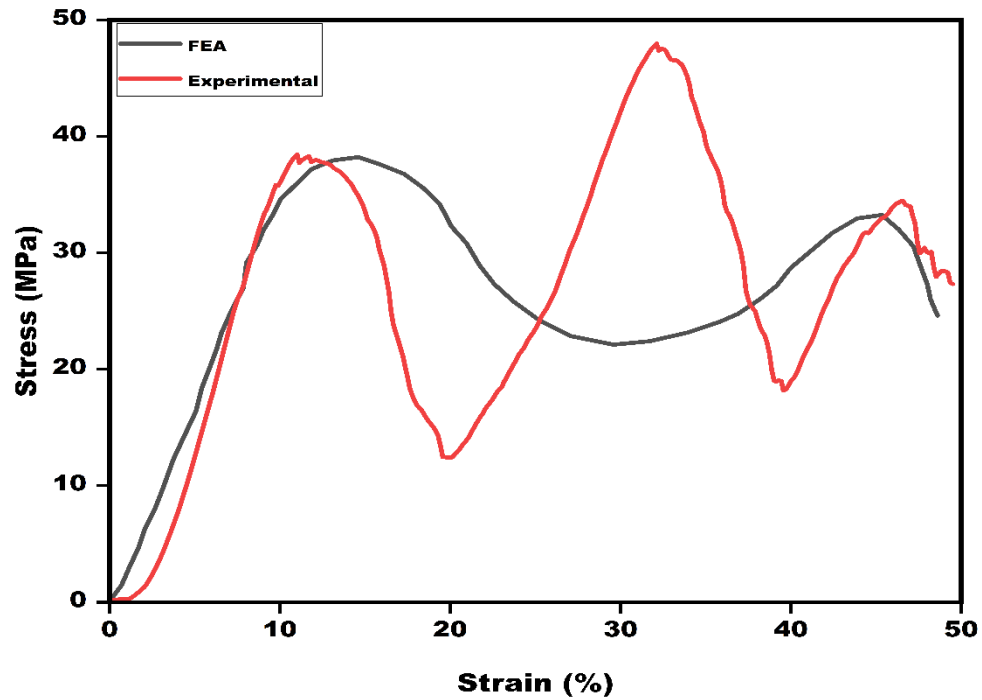


Figure 27: Experimental and FEA curves of compression test

Using experimental results and a matching numerical simulation, the nominal stress-strain curves for compression testing are displayed in Fig. 14. The numerically derived curves strongly indicate the accuracy of the FEA models as they agree well with the experimental data. As shown in **Fig.14** the experimental curve of the compression test represents considerable repeatability, and the numerical curves give considerable agreement with experimental results. The numerical peaks are hence slightly higher than the experimental values, owing to the relatively perfect numerical model which has not considered these imperfections. **Fig.15** represents the struts' buckling behavior experimentally and numerically with time. Similarly, the regions in the struts near point O or face sheets always present relatively high-stress levels and can be regarded as plastic hinges. The buckling failure is susceptible to initiation from these plastic hinges and agrees well with the experimental observation in **Figs.8** and **11**.

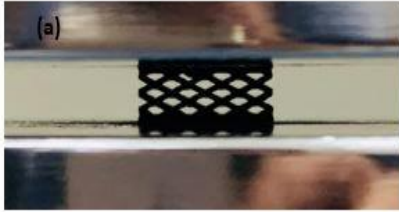
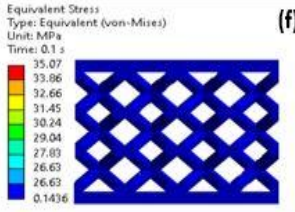
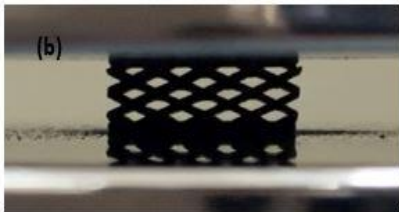
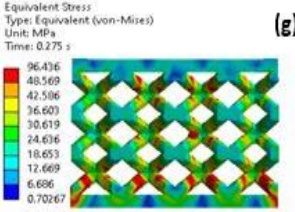

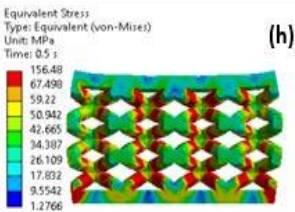

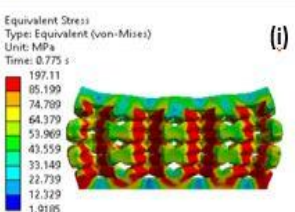

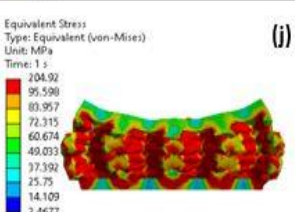
Time(sec)	Experiment	FEA
0.1		 <p>Equivalent Stress Type: Equivalent (von-Mises) Unit: MPa Time: 0.1 s</p> <p>35.07 33.96 32.66 31.45 30.24 29.04 27.83 26.63 26.63 0.1436</p>
0.275		 <p>Equivalent Stress Type: Equivalent (von-Mises) Unit: MPa Time: 0.275 s</p> <p>96.436 48.569 42.586 36.603 30.619 24.636 18.653 12.669 6.686 0.70267</p>
0.5		 <p>Equivalent Stress Type: Equivalent (von-Mises) Unit: MPa Time: 0.5 s</p> <p>156.48 67.498 59.22 50.942 42.665 34.387 26.109 17.832 9.5542 1.2766</p>
0.775		 <p>Equivalent Stress Type: Equivalent (von-Mises) Unit: MPa Time: 0.775 s</p> <p>197.11 85.199 74.789 64.379 53.969 43.559 33.149 22.739 12.329 1.9185</p>
1		 <p>Equivalent Stress Type: Equivalent (von-Mises) Unit: MPa Time: 1 s</p> <p>204.92 95.598 83.957 72.315 60.674 49.033 37.392 25.75 14.109 2.4677</p>

Figure 28:(a)-(e)Experimental compression test specimen behavior: From (f)-(j) compression specimen FEA

The load-deflection curves for three-point bending tests, together with the associated numerical simulation and experimental results, are displayed in Fig. 16. Similar to the compression findings, there is a notable degree of repeatability in the experimental data, and the numerical curves corroborate the experimental results. As shown in Fig.17. A vertical load is applied at the middle of the top face sheet and gradually increases downwards at a rate of 2mm/minute. The results of the experiment and the computer analysis demonstrate that the struts under the punch buckle and subsequently deform significantly. The stress of the struts beneath the punch, as shown



in Fig. 17, is much higher than that of other struts, confirming the experimental finding that strut failure typically happens here. These findings unequivocally demonstrate the *method by which the connections between the struts and the face sheets are always made when the Kagome lattice structures collapse under compression.*

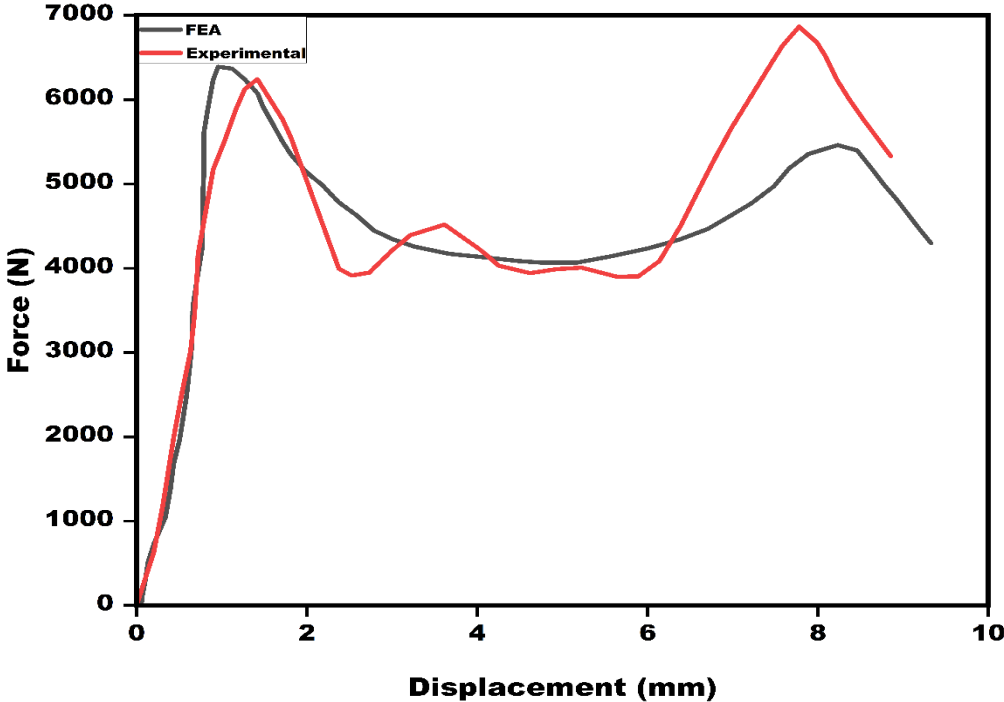


Figure 29: Experimental and FEA curves of three-point bending test

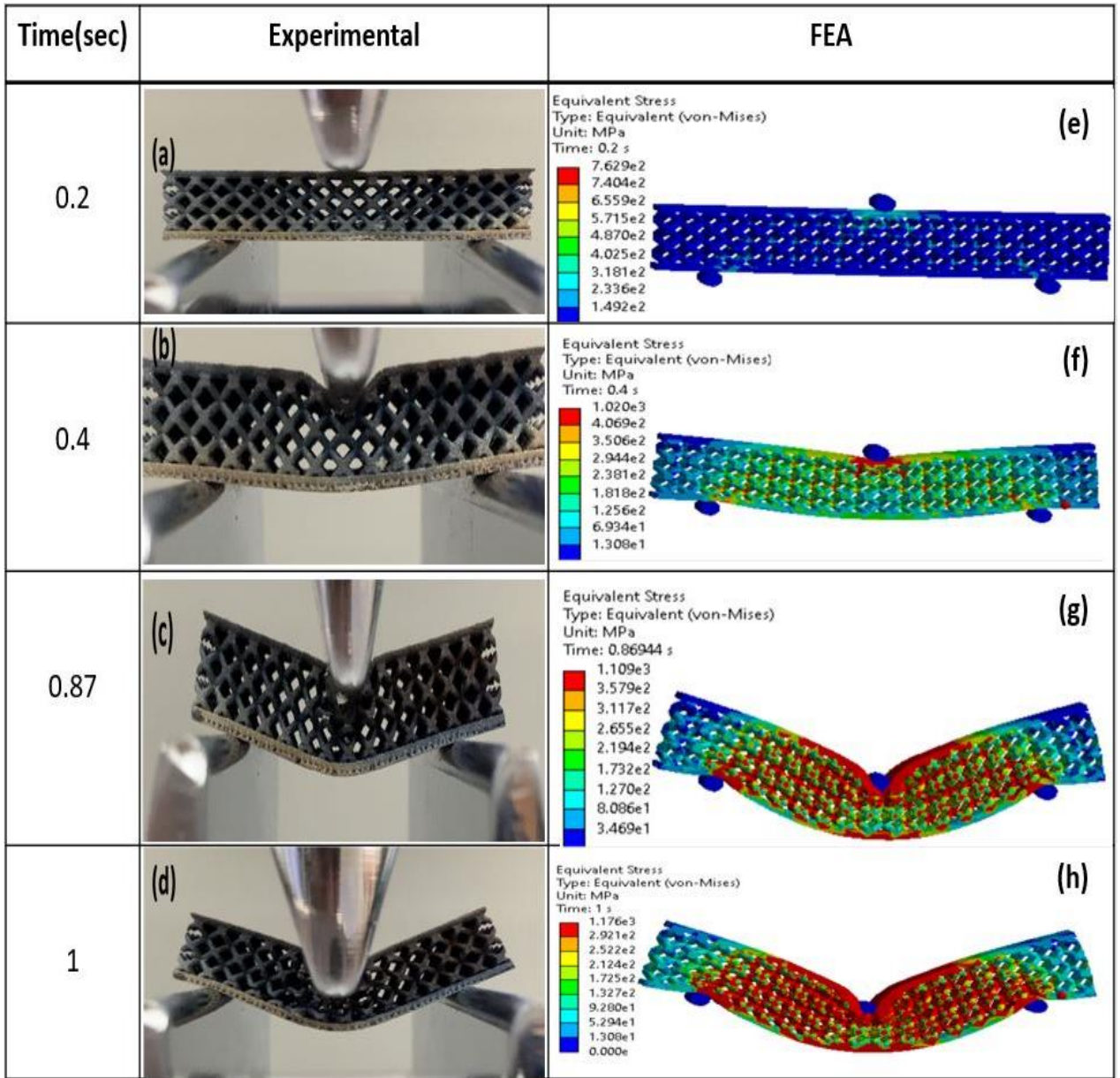


Figure 30: From (a)-(d) Experimental three-point bending test specimen setup; from (e)-(h) Numerical analysis of three-point bending test specimen.

#### 4.7 Conclusion

This work illustrates how versatile additive manufacturing can be when it comes to producing complicated structures because of its design flexibility. Lightweight 3D BCC lattice

sandwich structures were created and successfully fabricated. The mechanical qualities of the BCC lattice structure, including stiffness, energy absorption, and load carrying capability, were greatly enhanced via additive manufacturing. Numerical modeling and systematic experiments were performed to investigate the mechanical responses under three-point bending tests and compression. The findings of the numerical modeling demonstrated that face sheet wrinkling and strut buckling were the primary causes of failure in the BCC lattice sandwich constructions. The numerical modeling also showed that the initial bending support and other randomly distributed flaws created by the SLM process, including dedond between the struts and face sheet, had an impact on the compressive responses of the BCC lattice sandwich structures.

During compression, the primary mode of deformation is strut buckling, followed by fracture failure. Large deformation of the struts near the top face-sheet and modest displacement of the bottom face-sheets occurs from the struts beneath the punch in the lattice sandwich being more susceptible to buckling during bending. The findings of the numerical modeling demonstrated that face sheet wrinkling and strut buckling were the primary causes of failure in the BCC lattice sandwich constructions.

Functionally graded lattice density has brought an enormous opportunity in designing lightweight and robust parts. In comparison to a homogeneous lattice construction, the average bending load capacity improves from 6000.0 N to 16000.0 N due to the functionally graded lattice, which also exhibits stiff behavior. These findings suggest that functionally graded lattice architectures are amenable to widening and widespread application in the production of high-performance components for many sectors.

The study demonstrated that the SLM process could be used to fabricate BCC lattice sandwich structures with high mechanical properties, and the numerical modelling could provide insights into the structures' failure mechanisms and deformation modes. The study also suggested that the BCC lattice sandwich structures could be used in various applications, such as lightweight structures, energy absorption devices, and impact-resistant structures.

The mechanical properties of the BCC lattice structure can still be investigated by adjusting the geometrical parameters, such as the thickness of the face sheet, the struts' slenderness ratio, the unit cell size, and the span length. A wide range of failure models can be used, such as buckling or plastic yield in the struts, shrinking and buckling in the face sheets, and so on. In addition, a new kind of functionally graded lattice structure may be created by mixing materials or changing the curvature of the struts. In addition, different types of periodic unit cells can be

connected to form a hybrid structure that enhances the mechanical performance and multifunctionalities of the design.

## References

- [1] I. Gibson *et al.*, *Additive manufacturing technologies*. Springer, 2021.
- [2] K. V. Wong and A. Hernandez, "A review of additive manufacturing," *International scholarly research notices*, vol. 2012, 2012.
- [3] D. Herzog, V. Seyda, E. Wycisk, and C. Emmelmann, "Additive manufacturing of metals," *Acta Materialia*, vol. 117, pp. 371-392, 2016.
- [4] M. Smith, Z. Guan, and W. J. Cantwell, "Finite element modelling of the compressive response of lattice structures manufactured using the selective laser melting technique," *International Journal of Mechanical Sciences*, vol. 67, pp. 28-41, 2013.
- [5] S. H. Riza, S. H. Masood, R. A. R. Rashid, and S. Chandra, "Selective laser sintering in biomedical manufacturing," in *Metallic Biomaterials Processing and Medical Device Manufacturing*: Elsevier, 2020, pp. 193-233.
- [6] T. Maconachie *et al.*, "SLM lattice structures: Properties, performance, applications and challenges," *Materials & Design*, vol. 183, p. 108137, 2019.
- [7] I. Yadroitsev, P. Krakhmalev, and I. Yadroitsava, "Selective laser melting of Ti6Al4V alloy for biomedical applications: Temperature monitoring and microstructural evolution," *Journal of Alloys and Compounds*, vol. 583, pp. 404-409, 2014.
- [8] B. Blakey-Milner *et al.*, "Metal additive manufacturing in aerospace: A review," *Materials & Design*, vol. 209, p. 110008, 2021.
- [9] J.-P. Kruth, M. Badrossamay, E. Yasa, J. Deckers, L. Thijs, and J. Van Humbeeck, "Part and material properties in selective laser melting of metals," pp. 3-14: Shanghai Jiao Tong Univ Press.
- [10] A. K. Singla *et al.*, "Selective laser melting of Ti6Al4V alloy: Process parameters, defects and post-treatments," *Journal of Manufacturing Processes*, vol. 64, pp. 161-187, 2021.
- [11] S. Waqar, Q. Sun, J. Liu, K. Guo, and J. Sun, "Numerical investigation of thermal behavior and melt pool morphology in multi-track multi-layer selective laser melting of the 316L steel," *The International Journal of Advanced Manufacturing Technology*, vol. 112, pp. 879-895, 2021.
- [12] L. J. Kumar and C. G. Krishnadas Nair, "Current trends of additive manufacturing in the aerospace industry," *Advances in 3D printing & additive manufacturing technologies*, pp. 39-54, 2017.
- [13] S.-H. Park, S.-J. Son, S.-B. Lee, J.-H. Yu, S.-J. Ahn, and Y.-S. Choi, "Surface machining effect on material behavior of additive manufactured SUS 316L," *Journal of Materials Research and Technology*, vol. 13, pp. 38-47, 2021.
- [14] M. E. Orme *et al.*, "Additive manufacturing of lightweight, optimized, metallic components suitable for space flight," *Journal of Spacecraft and Rockets*, vol. 54, no. 5, pp. 1050-1059, 2017.
- [15] S. Salunkhe and D. Rajamani, "Current trends of metal additive manufacturing in the defense, automobile, and aerospace industries," in *Advances in Metal Additive Manufacturing*: Elsevier, 2023, pp. 147-160.
- [16] M. K. Islam, P. J. Hazell, J. P. Escobedo, and H. Wang, "Biomimetic armour design strategies for additive manufacturing: A review," *Materials & Design*, vol. 205, p. 109730, 2021.
- [17] E. Anderson, "Additive Manufacturing in China: Aviation and Aerospace Applications (Part 2)," *Additive manufacturing in the aerospace industry*, 2013.
- [18] C. Laser, "A World First: Additively Manufactured Titanium Components Now Onboard the Airbus A350 XWB," *Additive Manufacturing Amazing*, 2014.
- [19] B. Kianian, "Wohlers report 2017: 3d printing and additive manufacturing state of the industry, annual worldwide progress report: Chapters titles: The middle east, and other countries," 2017.

- [20] R. V. Petrescu *et al.*, "Lockheed martin-a short review," *Journal of Aircraft and Spacecraft Technology*, vol. 1, no. 1, 2017.
- [21] *Titanium 3D Printing*. Available: <https://all3dp.com/1/3d-printing-titanium-methods-printers-applications/>
- [22] L. Nickels, "AM and aerospace: an ideal combination," *Metal Powder Report*, vol. 70, no. 6, pp. 300-303, 2015.
- [23] A. L. R. Prathyusha and G. R. Babu, "A review on additive manufacturing and topology optimization process for weight reduction studies in various industrial applications," *Materials Today: Proceedings*, vol. 62, pp. 109-117, 2022.
- [24] L. Berrocal *et al.*, "Topology optimization and additive manufacturing for aerospace components," *Progress in Additive Manufacturing*, vol. 4, pp. 83-95, 2019.
- [25] J. Plocher and A. Panesar, "Review on design and structural optimisation in additive manufacturing: Towards next-generation lightweight structures," *Materials & Design*, vol. 183, p. 108164, 2019.
- [26] S. Mohd Yusuf, S. Cutler, and N. Gao, "The impact of metal additive manufacturing on the aerospace industry," *Metals*, vol. 9, no. 12, p. 1286, 2019.
- [27] B. Barroqueiro, A. Andrade-Campos, R. A. F. Valente, and V. Neto, "Metal additive manufacturing cycle in aerospace industry: A comprehensive review," *Journal of Manufacturing and Materials Processing*, vol. 3, no. 3, p. 52, 2019.
- [28] S. Singamneni, L. V. Yifan, A. Hewitt, R. Chalk, W. Thomas, and D. Jordison, "Additive manufacturing for the aircraft industry: a review," *J. Aeronaut. Aerosp. Eng.*, vol. 8, no. 1, pp. 351-371, 2019.
- [29] T. W. Simpson, C. B. Williams, and M. Hripko, "Preparing industry for additive manufacturing and its applications: Summary & recommendations from a National Science Foundation workshop," *Additive Manufacturing*, vol. 13, pp. 166-178, 2017.
- [30] J. C. Najmon, S. Raeisi, and A. Tovar, "Review of additive manufacturing technologies and applications in the aerospace industry," *Additive manufacturing for the aerospace industry*, pp. 7-31, 2019.
- [31] B. Mueller, "Additive manufacturing technologies—Rapid prototyping to direct digital manufacturing," *Assembly Automation*, vol. 32, no. 2, 2012.
- [32] R. Snell *et al.*, "Methods for rapid pore classification in metal additive manufacturing," *Jom*, vol. 72, pp. 101-109, 2020.
- [33] W. Li, K. Yang, S. Yin, X. Yang, Y. Xu, and R. Lupoi, "Solid-state additive manufacturing and repairing by cold spraying: A review," *Journal of materials science & technology*, vol. 34, no. 3, pp. 440-457, 2018.
- [34] N. Tuncer and A. Bose, "Solid-state metal additive manufacturing: a review," *Jom*, vol. 72, no. 9, pp. 3090-3111, 2020.
- [35] M. Srivastava, S. Rathee, S. Maheshwari, A. Noor Siddiquee, and T. K. Kundra, "A review on recent progress in solid state friction based metal additive manufacturing: friction stir additive techniques," *Critical Reviews in Solid State and Materials Sciences*, vol. 44, no. 5, pp. 345-377, 2019.
- [36] H. Taheri, M. R. B. M. Shoaib, L. W. Koester, T. A. Bigelow, P. C. Collins, and L. J. Bond, "Powder-based additive manufacturing—a review of types of defects, generation mechanisms, detection, property evaluation and metrology," *International Journal of Additive and Subtractive Materials Manufacturing*, vol. 1, no. 2, pp. 172-209, 2017.
- [37] H. Fayazfar *et al.*, "A critical review of powder-based additive manufacturing of ferrous alloys: Process parameters, microstructure and mechanical properties," *Materials & Design*, vol. 144, pp. 98-128, 2018.
- [38] S. Yuan, F. Shen, C. K. Chua, and K. Zhou, "Polymeric composites for powder-based additive manufacturing: Materials and applications," *Progress in Polymer Science*, vol. 91, pp. 141-168, 2019.

- [39] F. Wang and F. Wang, "Liquid resins-based additive manufacturing," *Journal of Molecular and Engineering Materials*, vol. 5, no. 02, p. 1740004, 2017.
- [40] S. Kumar, *Additive manufacturing processes*. Springer, 2020.
- [41] Y. Wang, Y. Zhou, L. Lin, J. Corker, and M. Fan, "Overview of 3D additive manufacturing (AM) and corresponding AM composites," *Composites Part A: Applied Science and Manufacturing*, vol. 139, p. 106114, 2020.
- [42] S. Kumar and S. Kumar, "Liquid based additive layer manufacturing," *Additive Manufacturing Processes*, pp. 131-145, 2020.
- [43] A. Kafle, E. Luis, R. Silwal, H. M. Pan, P. L. Shrestha, and A. K. Bastola, "3D/4D Printing of polymers: Fused deposition modelling (FDM), selective laser sintering (SLS), and stereolithography (SLA)," *Polymers*, vol. 13, no. 18, p. 3101, 2021.
- [44] K. Munir, A. Biesiekierski, C. Wen, and Y. Li, "Metallic biomaterials processing and medical device manufacturing," *Woodh Publ Ser Biomater*, vol. 235, p. 1, 2020.
- [45] I. A. Pelevin *et al.*, "Selective laser melting of Al-based matrix composites with Al<sub>2</sub>O<sub>3</sub> reinforcement: Features and advantages," *Materials*, vol. 14, no. 10, p. 2648, 2021.
- [46] C. Haase *et al.*, "Exploiting process-related advantages of selective laser melting for the production of high-manganese steel," *Materials*, vol. 10, no. 1, p. 56, 2017.
- [47] P. Religa, J. Rajewski, and P. Gierycz, "Advantages and Disadvantages of SLM and PIM Systems Used for Chromium (III) Separation from Aqueous Solutions," *Polish Journal of Environmental Studies*, vol. 24, no. 3, 2015.
- [48] P. Keller and R. Mendricky, "Parameters influencing the precision of SLM production," *MM Science Journal*, vol. 10, 2015.
- [49] R. Subbiah, J. Bensingh, A. Kader, and S. Nayak, "Influence of printing parameters on structures, mechanical properties and surface characterization of aluminium alloy manufactured using selective laser melting," *The International Journal of Advanced Manufacturing Technology*, vol. 106, pp. 5137-5147, 2020.
- [50] A. M. Khorasani, I. Gibson, M. Goldberg, and G. Littlefair, "A survey on mechanisms and critical parameters on solidification of selective laser melting during fabrication of Ti-6Al-4V prosthetic acetabular cup," *Materials & Design*, vol. 103, pp. 348-355, 2016.
- [51] M. Speirs *et al.*, "The effect of SLM parameters on geometrical characteristics of open porous NiTi scaffolds."
- [52] B. Barroqueiro, A. Andrade-Campos, and R. A. F. Valente, "Designing self supported SLM structures via topology optimization," *Journal of Manufacturing and Materials Processing*, vol. 3, no. 3, p. 68, 2019.
- [53] Solidwork. *3D CAD software*. Available: <https://www.solidworks.com>
- [54] nTopology. *Design the future with additive manufacturing*. Available: <https://www.ntop.com/>
- [55] W. Tao and M. C. Leu, "Design of lattice structure for additive manufacturing," pp. 325-332: IEEE.
- [56] B. K. Nagesha, V. Dhinakaran, M. V. Shree, K. P. M. Kumar, D. Chalawadi, and T. Sathish, "Review on characterization and impacts of the lattice structure in additive manufacturing," *Materials Today: Proceedings*, vol. 21, pp. 916-919, 2020.
- [57] Y. Tang, G. Dong, Q. Zhou, and Y. F. Zhao, "Lattice structure design and optimization with additive manufacturing constraints," *IEEE Transactions on Automation Science and Engineering*, vol. 15, no. 4, pp. 1546-1562, 2017.
- [58] A. Seharing, A. H. Azman, and S. Abdullah, "A review on integration of lightweight gradient lattice structures in additive manufacturing parts," *Advances in Mechanical Engineering*, vol. 12, no. 6, p. 1687814020916951, 2020.
- [59] P. Wang *et al.*, "Anisotropic compression behaviors of bio-inspired modified body-centered cubic lattices validated by additive manufacturing," *Composites Part B: Engineering*, vol. 234, p. 109724, 2022.



- [60] P. Wang, F. Yang, P. Li, B. Zheng, and H. Fan, "Design and additive manufacturing of a modified face-centered cubic lattice with enhanced energy absorption capability," *Extreme Mechanics Letters*, vol. 47, p. 101358, 2021.
- [61] S. Wang, J. Wang, Y. Xu, W. Zhang, and J. Zhu, "Compressive behavior and energy absorption of polymeric lattice structures made by additive manufacturing," *Frontiers of Mechanical Engineering*, vol. 15, pp. 319-327, 2020.
- [62] A. O. Aremu *et al.*, "A voxel-based method of constructing and skinning conformal and functionally graded lattice structures suitable for additive manufacturing," *Additive Manufacturing*, vol. 13, pp. 1-13, 2017.
- [63] M. Alaña, A. Lopez-Arancibia, A. Pradera-Mallabiarrena, and S. R. de Galarreta, "Analytical model of the elastic behavior of a modified face-centered cubic lattice structure," *Journal of the Mechanical Behavior of Biomedical Materials*, vol. 98, pp. 357-368, 2019.
- [64] D. Li, W. Liao, N. Dai, G. Dong, Y. Tang, and Y. M. Xie, "Optimal design and modeling of gyroid-based functionally graded cellular structures for additive manufacturing," *Computer-Aided Design*, vol. 104, pp. 87-99, 2018.
- [65] F. Teng, Y. Sun, S. Guo, B. Gao, and G. Yu, "Topological and Mechanical Properties of Different Lattice Structures Based on Additive Manufacturing," *Micromachines*, vol. 13, no. 7, p. 1017, 2022.
- [66] L. Yang, R. Mertens, M. Ferrucci, C. Yan, Y. Shi, and S. Yang, "Continuous graded Gyroid cellular structures fabricated by selective laser melting: Design, manufacturing and mechanical properties," *Materials & Design*, vol. 162, pp. 394-404, 2019.
- [67] N. Wang, G. K. Meenashisundaram, S. Chang, J. Y. H. Fuh, S. T. Dheen, and A. S. Kumar, "A comparative investigation on the mechanical properties and cytotoxicity of Cubic, Octet, and TPMS gyroid structures fabricated by selective laser melting of stainless steel 316L," *Journal of the Mechanical Behavior of Biomedical Materials*, vol. 129, p. 105151, 2022.
- [68] Y. Liu, Z. Dong, J. Ge, X. Lin, and J. Liang, "Stiffness design of a multilayer arbitrary BCC lattice structure with face sheets," *Composite Structures*, vol. 230, p. 111485, 2019.
- [69] Farsoon FS421M Available: <https://www.farsoon-gl.com>
- [70] "ASTM E8/8M, Standard test methods for tension testing of metallic materials.," ASTM International, West Conshohocken 2016, Available: <https://www.astm.org/>.
- [71] Z. Wang and P. Li, "Characterisation and constitutive model of tensile properties of selective laser melted Ti-6Al-4V struts for microlattice structures," *Materials Science and Engineering: A*, vol. 725, pp. 350-358, 2018.
- [72] "ASTM C365, Standard test method for flatwise compressive properties of sandwich cores, ," ASTM International, West Conshohocken 2006, Available: <https://www.astm.org/>.
- [73] *ASTM C393, Standard Test Method for Core Shear Properties of Sandwich Constructions by Beam Flexure.* . Available: <https://www.astm.org/>
- [74] H. Y. Sarvestani, A. H. Akbarzadeh, A. Mirbolghasemi, and K. Hermenean, "3D printed meta-sandwich structures: Failure mechanism, energy absorption and multi-hit capability," *Materials & Design*, vol. 160, pp. 179-193, 2018.
- [75] R. Goodall *et al.*, "The effects of defects and damage in the mechanical behavior of Ti6Al4V lattices," *Frontiers in Materials*, vol. 6, p. 117, 2019.